CHEMMEDCHEM

CHEMISTRY ENABLING DRUG DISCOVERY

Accepted Article

Title: Structure-Activity and Structure-Toxicity Relationships of Novel Peptoid-Based Histone Deacetylase Inhibitors with Dual-Stage Antiplasmodial Activity

Authors: Marcel Karl Walter Mackwitz, Eva Hesping, Yevgeniya Antonova-Koch, Daniela Diedrich, Tamirat Gebru, Tina Skinner-Adams, Mary Clarke, Andrea Schöler, Laura Limbach, Thomas Kurz, Elizabeth Ann Winzeler, Jana Held, Katherine Andrews, and Finn Kristian Hansen

To be cited as: *ChemMedChem* 10.1002/cmdc.201800808

Link to VoR: http://dx.doi.org/10.1002/cmdc.201800808

A Journal of

ChemPubSoc Europe

WILEY-VCH

www.chemmedchem.org

WILEY-VCH

FULL PAPER

Structure-Activity and Structure-Toxicity Relationships of Novel Peptoid-Based Histone Deacetylase Inhibitors with Dual-Stage Antiplasmodial Activity

Marcel K. W. Mackwitz,[a] Eva Hesping,[b] Yevgeniya Antonova-Koch,[c] Daniela Diedrich,[d] Tamirat Gebru Woldearegai,[e] Tina Skinner-Adams,[b] Mary Clarke,[b] Andrea Schöler,[a] Laura Limbach,[d] Thomas Kurz,[d] Elizabeth A. Winzeler,[c] Jana Held,[e] Katherine T. Andrews,*[+b] and Finn K. Hansen*[+a]

[a] M. K. W. Mackwitz, A. Schöler, Prof. Dr. F. K. Hansen
Pharmaceutical/Medicinal Chemistry, Institute of Pharmacy, Medical Faculty
Leipzig University
Brüderstraße 34, 04103 Leipzig, Germany.
E-mail: finn.hansen@medizin.uni-leipzig.de

[b] E. Hesping, Assoc. Prof. Dr. T. Skinner-Adams, M. Clarke, Prof. Dr. K. T. Andrews
Griffith Institute for Drug Discovery,
Don Young Road, Nathan Campus, Griffith University, QLD 4111, Australia
E-mail: k.andrews@griffith.edu.au

[c] Dr. Y. Antonova-Koch, Prof. Dr. E. A. Winzeler
Department of Pediatrics, School of Medicine, University of California, San Diego, 9500 Gilman Drive 0741, La Jolla, CA 92093, United States

[d] Dr. D. Diedrich, L. Limbach, Prof. Dr. T. Kurz
Institute of Pharmaceutical and Medicinal Chemistry,Heinrich-Heine-University Düsseldorf, 40225 Düsseldorf, Germany.

[e] Dr. T. G.Woldearegai, Dr. J. Held
Institut für Tropenmedizin, Eberhard Karls Universität Tübingen, Wilhelmstraße 27, 72074 Tübingen, Germany.

[+] These authors contributed equally to this work as senior authors.

Abstract: Novel malaria intervention strategies are of great importance due to the development of drug resistance in malaria endemic countries. In this regard, histone deacetylases (HDACs) have emerged as new and promising malaria drug targets. In this work, we present the design, synthesis and biological evaluation of 20 novel HDAC inhibitors with antiplasmodial activity. Based on a previously discovered peptoid-based hit compound, we modified all regions of the peptoid scaffold by utilizing a one-pot multicomponent pathway and submonomer routes to gain a deeper understanding of the structure-activity as well as structure-toxicity relationships. Most compounds displayed potent activity against asexual blood stage *P. falciparum* parasites with IC_{50} values ranging from 0.0052-0.25 µM and promising selectivity over mammalian cells ($SI^{Pf3D7/HepG2}$: 170-1483). In addition, several compounds showed encouraging submicromolar activity against *P. berghei* exo-erythrocytic forms (*Pb*EEF). Our study led to the discovery of the hit compound (*N*-(2-(benzylamino)-2-oxoethyl)-*N*-(4-(hydroxycarbamoyl)benzyl)-4-*i*-propylbenzamide, **2h**) as a potent and parasite-specific dual-stage antiplasmodial HDAC inhibitor (IC_{50} (*Pf*3D7) = 0.0052 µM, IC_{50} (*Pb*EEF) = 0.016 µM).

Introduction

Malaria is a potentially life-threatening parasitic disease that is prevalent in many tropical and sub-tropical regions of the world. Malaria parasite infection results in more than 200 million clinical cases and greater than 400,000 deaths annually.[1] Children and pregnant women are the most at-risk populations,[2] with *Plasmodium falciparum* infection causing the highest mortality.[2] Although some progress has been made in the field of malaria vaccines,[3] vector control and antimalarial drugs continue to be the mainstays of malaria prevention and treatment.[3,4,5] Unfortunately, the efficacy of antimalarial drugs is threatened by the development of parasite resistance, including the current gold standard artemisinin-based combination therapies (ACTs).[1,6] It is therefore important to identify new antimalarial drug candidates in order to prime the antimalarial drug development pipeline. Histone deacetylase inhibitors (HDACi) are a promising new class of potential antimalarial drugs.[2,7] HDACi are usually applied for the epigenetic treatment of different types of cancer and four drugs have been FDA-approved (vorinostat, belinostat, romidepsin and panobinostat) for the treatment of T-cell lymphoma or multiple myeloma.[8] The scope of HDACi has been extended and this class of compounds is currently being intensively investigated in several non-cancer diseases such as neurodegenative diseases, inflammation, HIV and parasitic diseases.[9-10] Different *Plasmodium* species are highly sensitive to HDACi treatment (Figure 1) and histone deacetylases (HDACs) are therefore considered as emerging antimalarial drug targets.[2,7] HDAC encoding genes have been discovered in all *Plasmodium* species that can infect humans.[2,7] While there are 18 HDAC isoforms in humans, a recent study re-confirmed the presence of five *P. falciparum* histone deacetylases (*Pf*HDACs) and identified one novel putative *Pf*HDAC.[2,11b] Like the human homologues, *Pf*HDACs are divided into zinc dependent class I (*Pf*HDAC1) and class II HDACs (*Pf*HDAC2 and 3), and sirtuin-like

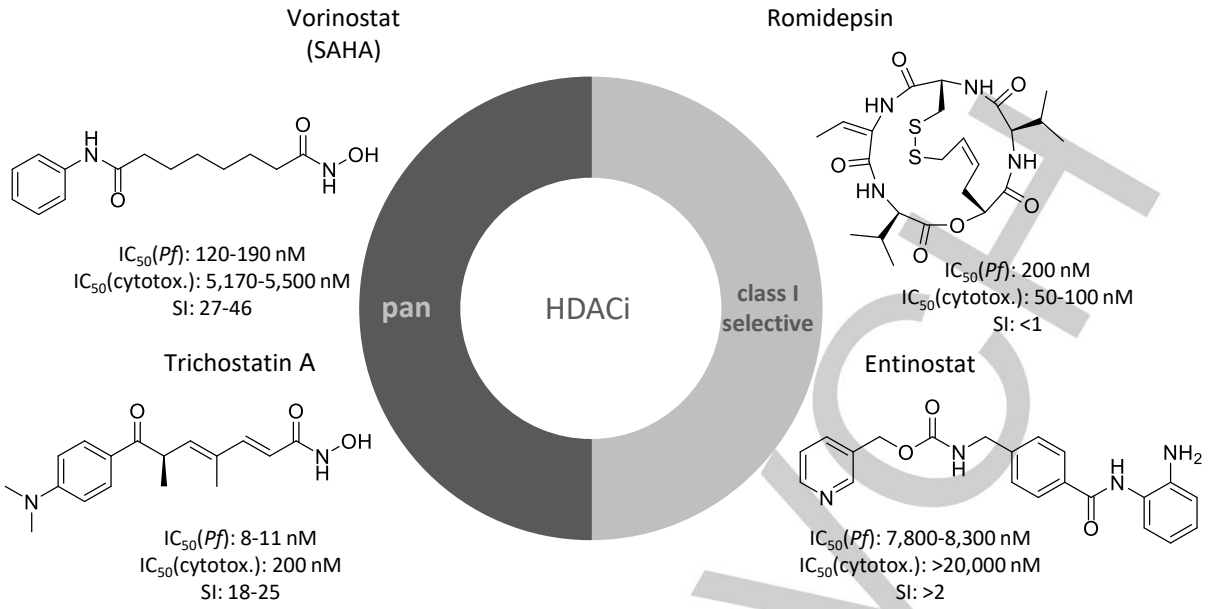

Figure 1. Selected HDACi and their antiplasmodial activity (*P. falciparum* = *Pf*), cytotoxicity (against mammalian cells) and selectivity indices (SI = IC_{50} (cytotox.))/IC_{50} (*Pf*)). Data are from references[2,14-15].

class III HDACs (*Pf*Sir2A and B).[2,11b] *Pf*HDAC1 possess a high sequence identity to its human class I homologues (61% to hHDAC1 and 62% to hHDAC2), and homology modelling studies show that the zinc-coordinating amino acids in HDACs and the tubular entrance between the zinc atom and the surface of the HDAC enzymes are well conserved between human class I HDAC enzymes and *Pf*HDAC1.[12-13] This might explain the sensitivity of *P. falciparum* to pan- and class I selective HDACi. However, pan- and class I-selective HDACi usually display significant toxicity against mammalian cells which leads to unsatisfactory selectivity against parasites versus human cells (Figure 1).[2,14-16] Another interesting finding regarding antiplasmodial HDACi is their activity against several malaria parasite life cycle stages. While most antimalarial drugs target just one specific life cycle stage (mostly asexual blood stages), several HDACi are also active against liver stages and late stage gametocytes.[5,17-18] This highlights the potential of HDACi as novel antiplasmodial agents.

In this regard, we, and others, hypothesized that class II selective hHDACi might be a better starting point for the development of parasite-selective antiplasmodial HDACi, due to their usually lower toxicity to mammalian cells.[5,17,19a] In addition, knock out experiments with the class IIb isozyme hHDAC6 in mice led to a viable phenotype with no significant defects.[19b] In a previous publication, starting from a hHDAC6 preferential scaffold,[20] we reported on the multicomponent synthesis and biological evaluation of novel peptoid-based antiplasmodial HDACi.[17] Several of these HDACi displayed potent activities against the 3D7 line of *P. falciparum* with IC_{50} values ranging from 4-158 nM and promising parasite-selectivity.[17] Furthermore, several compounds showed submicromolar activity against *P. berghei* exo-erythrocytic stages, making this novel type of HDACi an encouraging starting point for the development of antiplasmodial drug leads with dual stage activity.[17] The aim of this study was to gain a better insight into the structure-activity and structure-toxicity relationships of this new class of HDACi with antiplasmodial activity and in particular, to explore the structural requirements for potent dual-stage activity. Therefore, a series of analogues with a variety of structural variations were designed (Figure 2). In particular, we aimed for various modifications on the cap group, as well as truncation of the linker. Herein, we describe the synthesis and biological evaluation of a library of second-generation peptoid-based HDACi.

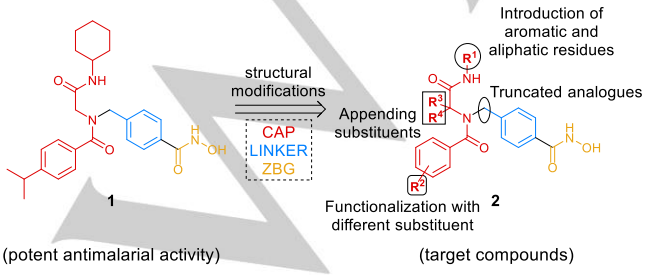

Figure 2. Design of target compounds.

Results and Discussion

Diversity-oriented synthesis of peptoid-based HDACi

The compounds described in this study are peptoid-based hydroxamic acids. To synthesize a mini-library of these target compounds, we applied two different diversity-oriented approaches: (1) the Ugi four component reaction (U-4CR, Scheme 1) and (2) submonomer pathways (Scheme 2). Most recently, we reported on the synthesis of peptoid-based HDACi by utilizing a microwave-assisted Ugi four-component reaction (U-4CR) in combination with a subsequent sodium methanolate/hydroxylamine hydrochloride based hydroxylaminolysis in a one-pot fashion to afford the desired

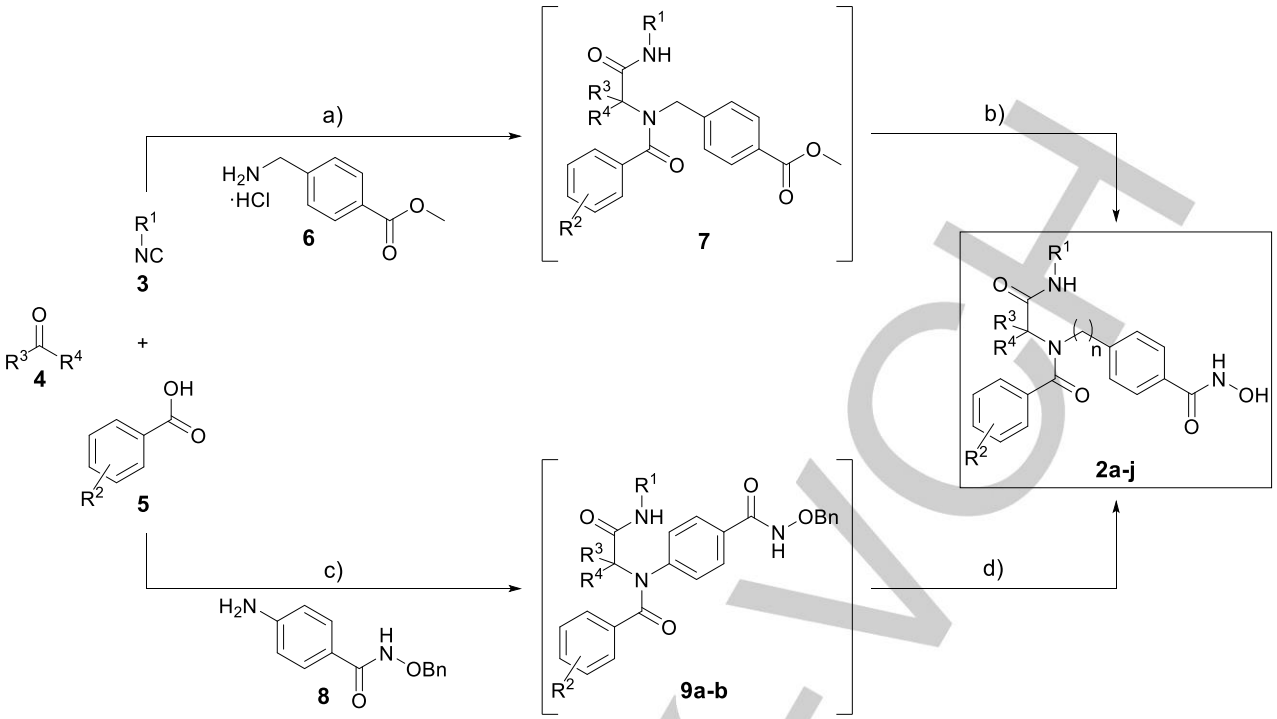

Scheme 1. Microwave-assisted multicomponent approach utilizing the Ugi four-component reaction to synthesize hydroxamic acids (**2a-j**). *Reagents and conditions:* a) (i) 4, 6, Et_3N, MeOH, 4 Å MS, 150 W, 45°C, 30 min; (ii) R^1-NC, R^2-COOH, 150 W, 45°C, 120 min; b) aq. H_2NOH, NaOH, DCM/MeOH (1:3), rt; c) MeOH, 4Å MS, rt, 72 h; d) MeOH, Pd/C, H_2, 2 h

hydroxamic acids of type **2**.[17] In this study, we aimed for a more convenient hydroxamic acid synthesis and applied an aqueous hydroxylaminolysis using aqueous hydroxylamine with sodium hydroxide as base, also in a one-pot multicomponent approach, thus avoiding the fresh preparation of methanolate (Scheme 1). Compounds **2c,e-h** were synthesized using this protocol in 11-88 % yield, while compound **2d,i-j** were prepared using the previously described protocol in 56-83 % yield.[17] The synthesis of the truncated derivatives **2a-b** was accomplished using the *O*-benzyl protected hydroxamic acid **8** as amine in the U-4CR (8-27 % yield) and subsequent deprotection by catalytic hydrogenolysis (23-54 % yield, Scheme 1), since the hydroxylaminolysis of the corresponding esters in the standard protocol did not produce the desired hydroxamic acids. Based on this synthetic approach, our peptoid-based hydroxamic acids can be structurally divided into an isocyanide (R^1), carboxylic acid (R^2), carbonyl (R^3 and R^4) and amine (n = 0 and 1) region.

Even though this multicomponent one-pot synthesis is efficient and versatile, it features some disadvantages. The U-4CR requires the use of isocyanides, which are mostly quite toxic, often possess a very unpleasant odor and the commercially available isocyanides are limited regarding chemical space. The typical synthetic strategy of isocyanides is the formamidation of the amine followed by dehydration, with the most common dehydration reagents (e.g. $POCl_3$) additionally having drawbacks due to their toxicity.[21] However, peptoids are also accessible by so-called submonomer pathways (Scheme 2). In this approach, three of the previously described regions (for instance the linker, carbonyl and carboxylic acid region) are kept unchanged, while one region can be varied in a diversity-oriented fashion. Therefore, we applied two submonomer pathways in order to derivatize the isocyanide (R^1) and carboxylic acid region (R^2). The synthesis of the target compounds **2k-t** is summarized in Scheme 2. Briefly, in the submonomer pathway 1, methyl 4-(aminomethyl)benzoate hydrochloride **6** was reacted with *t*-butyl bromoacetate (**10**, 46 % yield) and subsequently acylated with 3,5-dimethylbenzoyl chloride to afford *t*-butyl ester **11** in 99 % yield. After deprotection of the *t*-butyl group **11** (>99 %) and EDC-mediated amide coupling reactions (56-82 %) to afford intermediates **12k-r**, the desired hydroxamic acids **2k-r** were obtained by an aqueous hydroxylaminolysis using hydroxylamine and sodium hydroxide in 24-91 % yield. Hydroxamic acids **2s,t** were prepared via submonomer pathway 2 starting with a reaction of bromoacetyl bromide **13** with methylamine hydrochloride (46 %), followed by a substitution reaction with 4-(aminomethyl)benzoate hydrochloride **6** to afford the secondary amine **14** in 50 % yield. Thereafter, amine **14** was acylated with two different benzoyl chlorides to provide **15s,t**. Finally, the target compounds **2s,t** were synthesized in 40-86 % yield by hydroxylaminolysis of **15s,t** as described above.

In vitro inhibition of *P. falciparum* asexual intraerythrocytic parasite growth, cytotoxicity and parasite selectivity

The synthesized mini-library was tested for *in vitro* activity against asexual intraerythrocytic stage parasites as well as for cytotoxicity against human liver hepatocellular carcinoma cells (HepG2; Table 1). All compounds, except **2a**, **2b**, **2d** and **2i**, revealed potent activity (IC_{50} (*Pf*3D7): ≤ 0.25 µM) in combination with good parasite selectivity (selectivity index (SI) > 100) with IC_{50} values against the 3D7 line of *P. falciparum* ranging from 0.0052 to 0.25 µM and selectivity indices ranging from 170 to 1483. In contrast, the reference HDACi vorinostat (SAHA, IC_{50} (*Pf*3D7): 0.17 µM, IC_{50} (HepG2): 2.51 µM) showed only a low selectivity index of 15. Interestingly, the observed structure-activity (SARs) and structure-toxicity (STRs) relationships seem

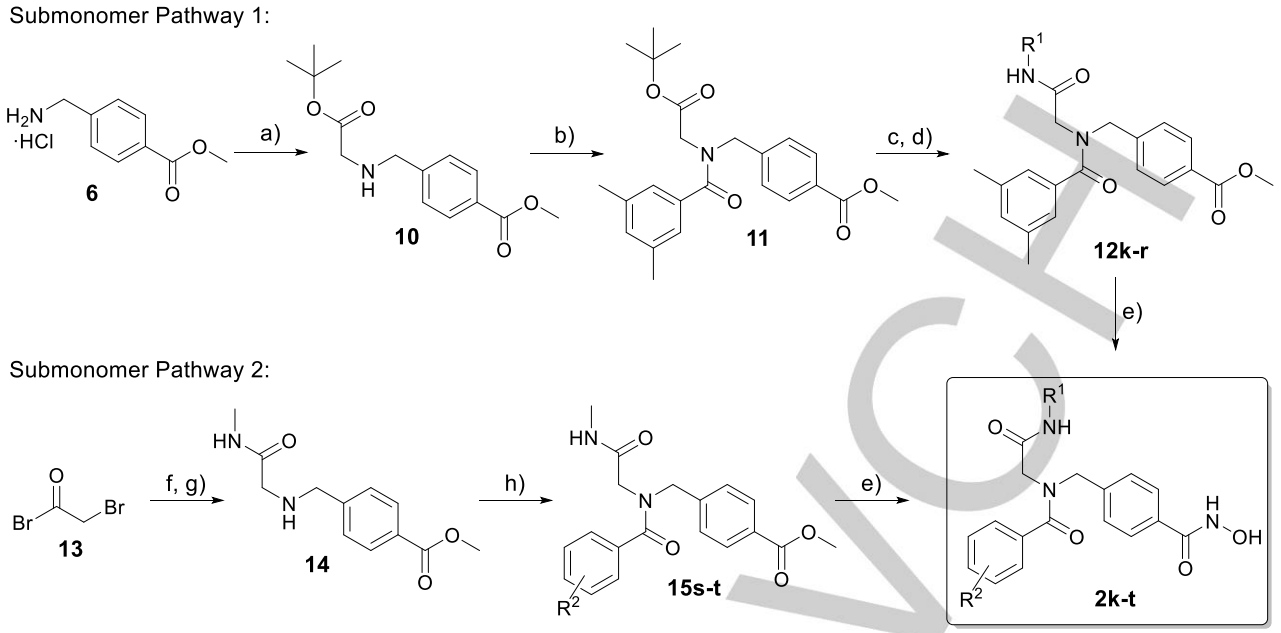

Scheme 2. Submonomer pathways for the synthesis of peptoid-based hydroxamic acids (**2k-t**). *Reagents and conditions:* a) *t*-Butyl bromoacetate, Et_3N, THF, rt, o.n.; b) 3,5-dimethylbenzoyl chloride, Et_3N, DCM, rt, o.n.; c) TFA/DCM (1:1), rt; d) R^1-NH_2, EDC, DMAP; Et_3N, DCM, rt, o.n.; e) aq. H_2NOH, NaOH, DCM/MeOH (1:3), rt, o.n.; f) methylamine hydrochloride, K_2CO_3, DCM, 3 h; g) methyl 4-(aminomethyl)benzoate hydrochloride **6**, Et_3N, THF, rt, o.n.; h) R^2-Ph-COCl, Et_3N, DCM, rt, o.n..

to be highly dependent on the nature of the different peptoid regions (see Figure 3). First, our aim was to investigate the impact of structural modifications at the α-carbon of the cap group as well as the linker lengths, hence varying the linker and the carbonyl region. Truncation of the linker length (n = 0) reduced the antiplasmodial activity, as seen in compound **2a,b** (IC_{50} (*Pf*3D7): 0.57-77.7 µM) and therefore does not seem to be a beneficial structural modification. The introduction of substituents in the carbonyl region (R^3, R^4) provided interesting results. While compounds **2c** and **2d** both displayed low toxicity (IC_{50} (HepG2): >50 µM), the sterically demanding phenyl residue in compound **2d** decreased the antiplasmodial activity (IC_{50} (*Pf*3D7): 0.39 µM) in comparison to its dimethyl substituted counterpart **2c** (IC_{50} (*Pf*3D7): 0.095 µM) [p = 0.0025]. Therefore, the introduction of small residues in the carbonyl region suggests improvement in toxicity, while retaining good antiplasmodial activity. Next, we observed high antiplasmodial activity for compounds bearing a benzyl residue (R^1) in the isocyanide region, hence we tried to gain a better insight by introducing several structural variations. Consequently, we modified the carboxylic region (R^2) and synthesized compounds **2g-j** which exhibited potent antiplasmodial activity in the single- to double-digit nanomolar range (IC_{50} (*Pf*3D7): 0.0052-0.037 µM). The compounds bearing branched alkyl groups in *p*-position of the carboxylic region (R^2), **2g** and **2h**, showed the highest potency (IC_{50} (*Pf*3D7): 0.0052-0.0088 µM, SI: 889-1483), while having moderate toxicity against mammalian cells (IC_{50} (HepG2): 5-13 µM). Compound **2h** (IC_{50} (*Pf*3D7): 0.0052 µM, SI: 889), bearing an *i*-propyl group (R^2), displayed antiplasmodial activity comparable to the reference compound chloroquine (IC_{50} (*Pf*3D7): 0.0068 µM). In contrast, the replacement of the *i*-propyl group (R^2) by the bioisosteric and more polar *N,N*-dimethylamino group (compound **2i**) distinctly increased toxicity against human cells, resulting in a decreased parasitic selectivity (IC_{50} (HepG2): 0.62 µM, SI: 64). We next tried to optimize the benzyl residue (R^1) by introducing several substituents (halogene, methoxy, alkyl groups) and a bioisosteric 3-picolyl group (**2j-r)**, while keeping the carboxylic region identical (R^2: 3,5-CH_3-Ph). Compound **2j** with potent activity and moderate toxicity (IC_{50} (*Pf*3D7): 0.037 µM, IC_{50} (HepG2): 9.57 µM, SI: 259) and no further substitution on the benzylic group (R^1) served as a reference. The results indicate, that substituents on the benzylic group (R^1) in general tend to decrease toxicity (IC_{50} (HepG2): 15-26 µM) slightly, while showing no clear SAR and STR. Notably, compound **2r**, which possesses a 3-picolyl R^1 residue, revealed low toxicity (IC_{50} (HepG2): 41.93 µM, SI: 530), but on the other hand also exhibited a significantly lower antiplasmodial activity (IC_{50} (*Pf*3D7): 0.079 µM) than its structurally related compound **2j** [p = 0.0175]. Furthermore, we introduced a methyl group into the isocyanide region (R^1) and synthesized compound **2s** and **2t**. Initially, we investigated the methyl based compound **2s** bearing a 3,5-dimethyl group (R^2) to have a comparison to the benzylic based compounds **2j-r**. Compound **2s** displayed an improved

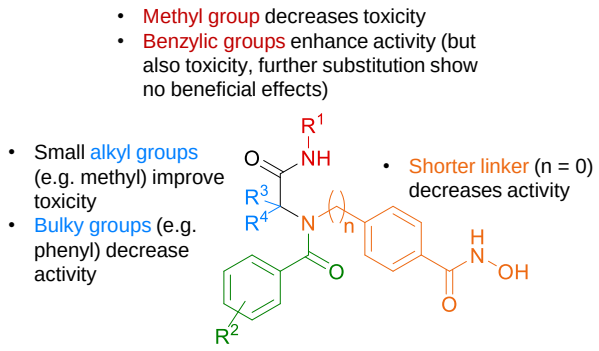

Figure 3. Structure-activity and -toxicity relationship of the peptoid-based hydroxamic acids.

toxicity profile against mammalian HepG2 cells (IC_{50} (HepG2): 47.98 µM, SI: 889) than hydroxamic acids **2j-r** (IC_{50} (HepG2): 9.57-41.93 µM, SI: 170-711), while keeping promising antiplasmodial activity (IC_{50} (*Pf*3D7): 0.054 µM). Accordingly, the small methyl group in the isocyanide region seems to have an impact on toxicity, which is also seen in compound **2t** (IC_{50} (HepG2): >50 µM, SI: >704). Notably, the introduction of substituents in the 2-position of the carboxylic region also lowers toxicity as seen in compounds **2e,f** (IC_{50} (HepG2): >50 µM), however, the antiplasmodial activity is simultaneously decreased as well (IC_{50} (*Pf*3D7): 0.11-0.25 µM).

Taken together, the substitution of the carboxylic region (R^2) has a strong influence on the antiplasmodial activity and especially branched alkyl groups, like the 4-*i*-propyl group, seem to have an enhancing effect.

Table 1. *In vitro* activity against asexual intraerythrocytic stage *P. falciparum* parasites, cytotoxicity and selectivity indices of **2a – 2t**.

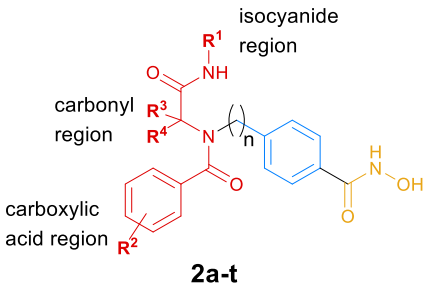

2a-t

2a-b: R^3 = H, R^4 = H, n = 0
2c: R^3 = CH_3, R^4 = CH_3, n = 1
2d: R^3 = Ph, R^4 = H, n = 1
2e-t: R^3 = H, R^4 = H, n = 1

Compound	R^1	R^2	*Pf* 3D7[a] IC_{50} [µM]	HepG2 IC_{50} [µM]	95% CI for HepG2 IC_{50}	SI[b]
2a	*c*-Hex	4-*i*-Pr	0.57(±0.089)	35.83	27.69-46.37	63
2b	*c*-Hex	3,5-CH_3	77.70(±7.94)	47.21	41.81-53.32	<1
2c	*c*-Hex	4-$(CH_3)_2N$	0.095(±0.015)	>50	n/a	>526
2d	*c*-Hex	4-$(CH_3)_2N$	0.39(±0.075)	>50	n/a	>128
2e	*t*-Bu	2-CH_3	0.11(±0.080)	>50	n/a	>455
2f	*t*-Bu	2-CH_3O	0.25(±0.14)	>50	n/a	>200
2g	Bn	4-*t*-Bu	0.0088(±0.0032)	13.05	9.48-17.97	1483
2h	Bn	4-*i*-Pr	0.0052(±0.0036)	4.62	2.48-8.58	889
2i	Bn	4-$(CH_3)_2N$	0.0097(±0.0029)	0.62	0.44-0.88	64
2j	Bn	3,5-CH_3	0.037(±0.012)	9.57	6.97-13.15	259
2k	4-CH_3-Bn	3,5-CH_3	0.042(±0.011)	14.59	10.75-19.79	347
2l	4-CH_3O-Bn	3,5-CH_3	0.033(±0.0090)	19.18	Very wide	581
2m	4-F-Bn	3,5-CH_3	0.087(±0.044)	20.38	16.79-24.74	234
2n	4-Cl-Bn	3,5-CH_3	0.094(±0.0073)	20.49	14.25-29.47	218
2o	4-*t*-Bu-Bn	3,5-CH_3	0.11(±0.019)	26.22	17.59-39.08	238
2p	3,5-CH_3-Bn	3,5-CH_3	0.077(±0.022)	20.19	17.65-23-09	262
2q	3-CH_3-Bn	3,5-CH_3	0.12(±0.048)	20.37	13.16-31.53	170
2r	3-Picolyl	3,5-CH_3	0.079(±0.018)	41.93	35.22-49.93	530
2s	CH_3	3,5-CH_3	0.054(±0.0029)	47.98	Very wide	889
2t	CH_3	2-CH_3	0.071(±0.015)	>50	n/a	>704
SAHA			0.17(±0.035)	2.51	1.63-3.86	15
Chloroquine			0.0068(±0.0023)			

[a] Three independent assays were carried out, each carried out in triplicate wells. [b] Selectivity index (SI) = (mammalian cell IC_{50})/(*P. falciparum* IC_{50}).

In our previous study, we could not identify any clear SAR for the isocyanide region, which is confirmed by the results in this study.[18] Nonetheless, the isocyanide region appears to play a certain role in the STR, with methyl groups having the most promising toxicity improvement. Additionally, modifications at the α-carbon of the cap group have effects on the toxicity as well. In that respect, the introduction of methyl groups in the carbonyl region is beneficial regarding the toxicity profile.

Inhibition of human HDAC1 and HDAC6

The result of the evaluation of the cytotoxicity of compounds **2a-t** against mammalian HepG2 cells revealed a broad toxicity profile from submicromolar IC_{50} values to no cytotoxicity (IC_{50} (HepG2): >50 µM), in which the different residues of the peptoid-based hydroxamic acids suggest certain structure-toxicity relationships. In general, pan- and class I selective human HDAC inhibitors seem to show increased toxicity. Thus, it has been hypothesized, that class IIb preferential inhibitors may decrease side effects, due to a *inter alia* more precise alteration of biological substrates in the cell.[17a,18,22] In that regard, we screened selected compounds in a biochemical assay against the class I isoform hHDAC1 and the class IIb isoform hHDAC6 using ZMAL (Z-Lys(Ac)-AMC) as substrate to investigate, if the toxicity against mammalian cells shows any correlation to the human HDAC isoform profile. We tested the six compounds with the lowest toxicity against HepG2 cells (**2c-f, 2s-t**), and the three compounds with highest activity against the 3D7 line of *P. falciparum* and moderate (**2g** and **2h**) to high (**2i**) cytotoxicity (see Table 2). Indeed, all compounds revealed potent activity against the hHDAC6 isoform with IC_{50} values ranging from 0.014 to 0.089 µM. On the contrary, we observed differences in the hHDAC1 activity. The compounds with low toxicity against HepG2 cells (**2c-f**, **2s-t**) demonstrated moderate to low hHDAC1 activity (IC_{50} (hHDAC1): 0.29-3.11 µM), while compounds **2g-i** displayed potent activity in the double-digit nanomolar range (IC_{50} (hHDAC1): 0.0077-0.034 µM) with similar activity against hHDAC1 and hHDAC6. Hence, the potent activity against the human class I hHDAC1 isoform seems to be a possible explanation for the increased toxicity of certain compounds against mammalian cells. Notably, compounds **2e-f, t** turned out to be promising selective hHDAC6 inhibitors (IC_{50} (hHDAC6): 0.032-0.051 µM, $SI^{HDAC1/HDAC6}$: 47-82), comparable to other known selective HDAC6i like ricolinostat ($SI^{HDAC1/HDAC6}$: 11), HPOB ($SI^{HDAC1/HDAC6}$: 25) and Tubastatin A ($SI^{HDAC1/HDAC6}$: 178).[22-23]

Effect of peptoid-based HDAC inhibitors on *P. falciparum* histone acetylation

Hyperacetylation analysis was carried out on compounds **2c, 2g, 2h, 2s** and **2t** (Figure 4). Treatment with **2s** resulted in the highest levels of hyperacetylation, causing a significant (~2-fold) relative density increase compared to the **3h-C** non-treatment control ($p < 0.01$; Figure 4) irrespective of whether the signal corresponding to H4 (~11 kDa) or total signal including cross reactive bands (H2B/H2Bv (~13-14 kDa); H2A.Z (~16 kDa) was used. None other the peptoid-based HDAC inhibitors caused a significant increase in acetylation signals (p <0.5; Figure 4). As expected, the HDAC inhibitor control, vorinostat, also caused significantly increased acetylation compared to the vehicle control ($p < 0.01$; Figure 4). It is not clear why **2s**, but not the other peptoid-based HDAC inhibitors in this series, caused histone hyperacetylation, however factors that need to be considered include differences in compound uptake and possible *P. falciparum* HDAC specificity. It needs to be noted that these data are only a snapshot of treating a single developmental stage (asexual trophozoites). There may be different effects on different developmental forms or life stages where expression levels of target proteins, or compound exposure dynamics, may vary and therefore influence the level of acetylation. Future work should include the investigation of potential acetylation changes in other life stages within the intraerythrocytic lifecycle as well as the investigation of acetylation alterations to other histones. The differences in acetylation levels shown here may be related to different target preferences and further analysis will be required, however this is complicated by the lack of recombinant *Pf*HDAC proteins.

Table 2. Activities of compounds **2c-i,s-t** and the reference HDACis SAHA, Ricolinostat, HPOB and Tubastatin A against human HDAC1 (hHDAC1) and HDAC6 (hHDAC6).

Compound	hHDAC1 IC_{50} [µM]	hHDAC6 IC_{50} [µM]	SI[a]
2c	0.45(±0.026)	0.089(±0.002)	5
2d	0.84(±0.095)	0.064(±0.007)	13
2e	2.41(±0.086)	0.051(±0.004)	47
2f	3.11(±0.308)	0.038(±0.004)	82
2g	0.034(±0.0064)	0.071(±0.007)	<1
2h	0.019(±0.0017)	0.051(±0.003)	<1
2i	0.0077(±0.0000095)	0.014(±0.0005)	<1
2s	0.29(±0.054)	0.044(±0.004)	7
2t	2.01(±0.137)	0.032(±0.001)	63
SAHA	0.082(±0.015)	0.055(±0.011)	2
Ricolinostat[b]	0.19(±0.022)	0.018(±0.003)	11
HPOB[b]	2.10(±0.23)	0.0085(±0.0090)	25
Tubastatin A[b]	2.49(±0.14)	0.014(±0.00061)	178

[a] Selectivity index (SI) = hHDAC1/hHDAC6. [b] Data from ref.[22-23].

***In vitro* activity against *P. berghei* exo-erythrocytic forms and stage V *P. falciparum* gametocytes.**

Our previous study revealed that several peptoid-based hydroxamic acids act as antiplasmodial compounds with dual-stage activity against asexual blood stages and liver stages (*P. berghei* exo-erythocytic forms, *Pb* EEF).[18] Liver stage activity is an interesting additional feature, since this might prevent the development of the disease and could be applied as chemoprotection. Therefore, all 20 compounds were screened for their activity against *P. berghei* exo-erythocytic forms. The results are summarized in Table 3. Nine compounds (**2g-m**, **p, q**) revealed submicromolar activity against *Pb* EEF with IC_{50} values ranging from 0.016 to 0.58 µM ($SI^{HepG2/Pb\ EEF}$: 23-289), while three out of these nine compounds displayed double-digit nanomolar activity **2h-j** (IC_{50} (*Pb* EEF): 0.016-0.073 µM). Interestingly, all of

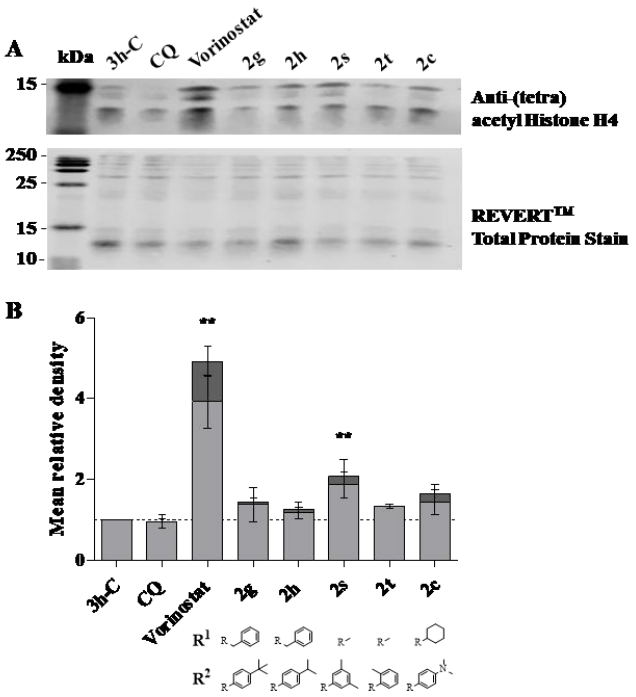

Figure 4. Hyperacetylation analysis of *P. falciparum* histone H4 by selected peptoid-based HDAC inhibitors. Western blot analysis of protein lysates prepared from trophozoite-stage *P. falciparum* 3D7 infected erythrocytes treated for 3 h with 5x IC_{50} of test or control compounds. Controls included a vehicle control (0.2 % DMSO; 3h-C), the non-HDAC inhibitor control chloroquine (CQ) and the positive HDAC inhibitor control vorinostat. (A) Western Blot was carried out using anti-(tetra)acetyl-histone H4 primary antibody and IRDye 680 goat anti-rabbit secondary antibody. Total protein per lane was detected using REVERT™ Total Protein Stain on the same membrane. Representative Western Blot shown. Protein molecular weight marker bands (kDa) are indicated. (B) Graph showing mean relative density (± SD) for three independent Western Blot experiments. Western signal densities were normalized to total protein load in the respective lane and expressed as fold change compared to the 3h-C DMSO vehicle control (taken as 1.0; dotted line). Data are mean (± SD) for three independent experiments. Significant differences are shown for H4 signal (~11 kDa; grey bars; ** $p < 0.01$) Total signal included H4 signal and cross reactive bands H2B/H2Bv (~13-14 kDa) and H2A.Z (~16 kDa).

the nine compounds with submicromolar activity bear a benzylic or substituted benzylic residue in the isocyanide region. However, the respective substitution in the carboxylic region seems to alter the activity drastically. The most promising derivative in regard to dual-stage activity was hydroxamic acid **2h** bearing a 4-*i*-propyl group in the carboxylic acid region (R^2), showing the highest activity both against *P. falciparum* asexual blood stages (*Pf* 3D7: 0.0052 µM; $SI^{HepG2/Pf\ 3D7}$: 889) and against *P. berghei* exo-erythocytic forms (IC_{50} (*Pb* EEF): 0.016 µM; $SI^{HepG2/Pb\ EEF}$: 289) in combination with encouraging parasite-selectivity.

Gametocytes are responsible for the transmission of the parasite to another host and targeting this life stage would contribute to the prevention of transmission, thus sooner or later eradicating the parasite. Hence, to further investigate the potential of these peptoid-based HDACi as multi-stage inhibitors, all compounds were screened for their activity against mature stage V *P. falciparum* gametocytes using an ATP bioluminescence assay. First, all compounds were screened at a fixed concentration of 5 µM. Subsequently, compounds with inhibitory activity in the primary screen were tested in dose response to determine IC_{50} values (Table 4).

Table 3. Activity of compounds **2a-t** against *P. berghei* exo-erythrocytic forms.

Compound	*Pb* EEF[a] IC_{50} [µM]	95% CI for *Pb* EEF IC_{50}	SI[b]
2a	9.70	5.20-18.09	4
2b	20.19	Very wide	2
2c	20.14	5.64-71.96	>3
2d	19.26	Very wide	>3
2e	9.70	4.08-23.05	>5
2f	26.69	11.13-63.97	>2
2g	0.58	0.28-1.20	23
2h	0.016	0.0080-0.031	289
2i	0.022	0.013-0.038	28
2j	0.073	0.044-0.12	131
2k	0.21	0.11-0.43	70
2l	0.57	0.32-1.02	34
2m	0.11	0.045-0.28	185
2n	1.00	0.33-3.00	21
2o	16.65	Very wide	2
2p	0.58	0.21-1.57	35
2q	0.13	0.066-0.24	157
2r	16.73	Very wide	3
2s	7.17	2.38-21.65	7
2t	28.05	9.54-82.53	>2
SAHA	0.0077	0.0055-0.011	326

[a] *P. berghei* exo-erythrocytic forms (*Pb* EEF). [b] Selectivity index (SI) = (mammalian cell IC_{50})/(Pb EEF IC_{50}). For HepG2 values (mammalian cell IC_{50}) see Table 1.

All compounds were found to have only moderate to poor activity against mature gametocytes (IC_{50} > 5 µM). The best activity was observed for compound **2p** (IC_{50} = 5.27 µM). It is an interesting finding that several compounds showed promising submicromolar activity against asexual blood stages and liver stages, but no noteworthy activity against mature gametocytes. The reason for this is currently unknown. However, this phenomenon could be related to an altered expression of the three zinc-dependent *Pf*HDACs in the different malaria parasite life cycle stages.

Conclusions

In conclusion, we synthesized a mini-library of 20 novel second generation peptoid-based HDACi. To this end, we applied efficient and diversity-oriented synthetic routes, which include a convenient one-pot Ugi multicomponent reaction and straightforward submonomer pathways. Based on our previous study, we derivatized all structural regions of the peptoid scaffold

Table 4. Activity of peptoid-based HDAC inhibitors against mature stage V *P. falciparum* gametocytes.

Compound	R^1	R^2	*Pf* stage V gametocytes[a] IC_{50} [µM]
2c	*c*-Hex	4-$(CH_3)_2$N-Ph	16.29(±5.99)
2d	*c*-Hex	4-$(CH_3)_2$N-Ph	14.81(±5.87)
2l	4-MeO-Bn	3,5-Me-Ph	10.21(±6.68)
2p	3,5-Me-Bn	3,5-Me-Ph	5.27(±3.39)
2s	Me	3,5-Me-Ph	16.84(±5.77)

[a] *P. falciparum* stage V gametocytes; at least two independent experiments, each in duplicate wells.

to get a better understanding of the structure-activity (SAR) and structure-toxicity relationships (STR). All synthesized compounds were screened and assessed for their antiplasmodial activity and human cell (HepG2) cytotoxicity. The majority of compounds displayed potent activity against asexual blood stage *P. falciparum* parasites (3D7 line) with IC_{50} values ranging from 0.0052-0.25 µM and selectivity indices over mammalian cells (HepG2) ranging from 170 to 1483. The results suggest that especially the carboxylic region (R^2) seems to have the greatest impact on SAR and STR, however, certain structural modification on the isocyanide (R^1) and carbonyl region ($R^{3,4}$) also possess beneficial effects regarding cytotoxicity improvement. Furthermore, all compounds were tested against mature stage V *P. falciparum* gametocytes and for activity against liver stage *P. berghei* exo-erythrocytic forms. Although only poor activity was observed against gametocytes, various compounds showed encouraging submicromolar activity against *P. berghei* exo-erythrocytic forms. Selected compounds were further screened for their inhibition of two representative human HDAC isoforms (hHDAC1 and 6), which indicated a correlation between higher cytotoxicity against human cells and increased activity against the human class I isoform hHDAC1. The most promising compound **2h** emerged as a potent dual-stage antiplasmodial HDACi (IC_{50} (*Pf* 3D7) = 0.0052 µM, IC_{50} (*Pb* EEF) = 0.016 µM) with parasite-specific activity. In addition, the biological evaluation led to several compounds (**2c**, **2e**, **2s**, **2t**) with promising antiplasmodial activity (IC_{50}(*Pf* 3D7) = 0.054-0.12 µM) and low cytotoxicity (IC_{50} (HepG2) = 47.98->50 µM, $SI^{Pf\ 3D7/HepG2}$ = >417-889). Thus, this series of compounds represent a valuable starting point for the development of novel drug candidates with potent dual-stage antiplasmodial activity and an optimized toxicity profile.

Experimental Section

Synthesis

All chemicals and solvents were obtained from commercial suppliers (Sigma-Aldrich, Acros Organics, Carbolution Chemicals) and used as purchased without further purification. All microwave-assisted reactions were carried out with a CEM Focused Microwave System, Model Discover. The progress of all reactions was monitored by thin layer chromatography (TLC) using Merck precoated silica gel plates (with fluorescence indicator UV_{254}). Components were visualized by irradiation with ultraviolet light (254 nm) or staining in potassium permanganate solution following heating. Flash column chromatography was performed using prepacked silica cartridge with the solvent mixtures specified in the corresponding experiment. Melting points (mp) were taken in open capillaries on a Mettler FP 5 melting-point apparatus and are uncorrected. Proton (^{1}H) and carbon (^{13}C) NMR spectra were recorded on a Bruker (Avance) or Varian (Mecury-plus) 300, 400, 500 or 600 using DMSO-d_6 or $CDCl_3$ as solvents. Chemical shifts are given in parts per million (ppm), relative to residual solvent peak for ^{1}H and ^{13}C. Due to the well-known phenomenon of cis/trans-amide bond rotamers in peptoids[20c], ^{1}H and ^{13}C NMR-signals can occur as two distinct sets of signals. ^{1}H NMR signals marked with an asterisk (*) correspond to peaks assigned to the minor rotamer conformation. High resolution mass spectra (HRMS) analysis was performed on a UHR-TOF maXis 4G, Bruker Daltonics, Bremen by electrospray ionization (ESI). Analytical HPLC analysis were carried out on a Knauer HPLC system equipped with a Knauer UV detector K-2600 (254nm) using a Vertex Plus Column (length 150 x 4 mm with precolumn, packing material of the column was Eurospher II 100-5 C18). UV absorption was detected at 254 nm with a isocratic gradient of 10% B to 100% B in 30 min using HPLC-grade water +0.1% TFA (solvent A) and HPLC-grade acetonitrile +0.1% TFA (solvent B) for elution at a flow rate of 1 mL/min. The purities of all final compounds were 95% or higher.

Synthesis of *N*-(2-(cyclohexylamino)-2-oxoethyl)-*N*-(4-(hydroxycarbamoyl)phenyl)-4- isopropylbenzamid 2a:

4-Amino-*N*-benzyloxy-benzamide was synthesized according to reference[24]. A mixture of 4-amino-*N*-benzyloxy-benzamide (436 mg, 1.8 mmol, 1 eq.), paraformaldehyde (66 mg, 2.26 mmol, 1.2 eq.) and 50 mg of crushed molecular sieves (MS) 4 Å in dry methanol (4 mL, 0.5 M) was stirred for 30 min at room temperature. Next, 4-*i*-propylbenzoic acid (**5a**, 296 mg, 1.8 mmol, 1 eq.) and cyclohexyl isocyanide (**3a**, 221 µL, 1.8 mmol, 1 eq.) was added and stirred for 72 h at room temperature. Subsequently, the solvent was removed under reduced pressure and the residue was dissolved in ethyl acetate (20 mL). The organic phase was washed with 1 M HCl (3 x 30 mL) and with sat. $NaHCO_3$/water (1:1, 3 x 20 mL). The organic phase was dried over sodium sulfate, filtered, and the solvent was removed under reduced pressure. The crude product was purified by flash column chromatography (dichloromethane/methanol, gradient) to yield the desired compound **9a** in 8 % yield as an brown oil: ^{1}H-NMR ($CDCl_3$, 300 MHz): δ [ppm] = 1.11-1.45 (m, 5 H), 1.19 (d, J = 6.9 Hz, 6 H), 1.56-1.75 (m, 3 H), 1.87-1.92 (m, 2 H), 2.76-2.90 (m, 1 H), 3.71-3.84 (m, 1 H), 4.45 (s, 2 H), 5.00 (s, 2 H), 6.37-6.40 (m, 1 H), 7.04-7.07 (m, 2 H), 7.12-7.15 (m, 2 H), 7.24-7.27 (m, 2 H), 7.38-7.45 (m, 5 H), 7.51-7.54 (m, 2 H), 8.86 (s, 1 H); ^{13}C-NMR ($CDCl_3$, 75 MHz): δ [ppm] = 23.8, 24.8, 25.6, 33.1, 34.1, 48.5, 55.1, 77.4, 78.5, 126.4, 127.1, 128.4, 128.8, 129.0, 129.3, 129.4, 130.2, 131.8, 135.3, 147.4, 152.1, 167.7, 171.3.; HRMS calculated for $C_{32}H_{37}N_3O_4$: 528.2859 $[M+H]^+$, found 528.2857.

Compound **9a** (146 mg, 0.28 mmol, 1 eq.) was dissolved in methanol (20 mL) and a catalytical amount of Pd/C (10wt. %) was added. Subsequently, the mixture was stirred for 2 h at room temperature under a hydrogen atmosphere. Next, the solution was filtered through pad of Celite and the solvent was removed under reduced pressure. After purification by flash column chromatography (dichloromethane/methanol, gradient), the desired product **2a** was obtained in 23 % yield as white solid: mp = 120 °C; ^{1}H-NMR ($CDCl_3$, 600 MHz): δ [ppm] = 1.14 (d, J = 6.9 Hz, 6 H), 1.17-1.36 (m, 5 H), 1.57-1.59 (m, 1 H), 1.66-1.69 (m, 2 H), 1.84-1.86 (m, 2 H), 2.77-2.84 (m, 1 H), 3.72-3.79 (m, 1 H), 4.48 (s, 2 H), 6.75-6.76 (m, 1 H), 7.02-7.08 (m, 4 H), 7.22-7.23 (m, 2 H), 7.55-7.56 (m, 2 H), 8.32 (brs, 1 H), 10.38 (s, 1 H); ^{13}C-NMR ($CDCl_3$, 151 MHz): δ [ppm] = 23.7, 24.7, 25.6, 32.9, 34.1, 48.6, 55.1, 126.4, 127.1, 128.3, 129.1, 129.4, 131.5, 146.9, 152.3, 164.7, 168.4, 171.6.; HRMS calculated for $C_{25}H_{31}N_3O_4$: 438.2387 $[M+H]^+$, found 438.2387; HPLC purity: 96.4 %.

Synthesis of *N*-(2-(cyclohexylamino)-2-oxoethyl)-*N*-(4-(hydroxycarbamoyl)phenyl)-3,5- dimethylbenzamide 2b:

4-Amino-*N*-benzyloxy-benzamide was synthesized according to reference[24]. A mixture of 4-amino-*N*-benzyloxy-benzamide (290 mg, 1.2 mmol, 1.2 eq.), paraformaldehyde (36 mg, 1.2 mmol, 1.2 eq.) and 50 mg of crushed molecular sieves (MS) 4 Å in dry methanol (4 mL, 0.5 M) was stirred for 30 min at room temperature. Next, 3,5-dimethylbenzoic acid (**5b**, 150 mg, 1.0 mmol, 1 eq.) and cyclohexyl isocyanide (**3a**, 122 µL, 1.0 mmol, 1 eq.) was added and stirred for 72 h at room temperature. Subsequently, the solvent was removed under reduced pressure and the residue was dissolved in ethyl acetate (20 mL). The organic phase was extracted with 1 M HCl (3 x 30 mL) and with sat. $NaHCO_3$/water (1:1, 3 x 20 mL). The organic phase was dried over sodium sulfate, filtered, and the solvent was removed under reduced pressure. The crude product was purified by flash column chromatography (dichloromethane/methanol, gradient) to yield the desired compound **9b** in 27 % yield as an oil: ^{1}H-NMR ($CDCl_3$, 300 MHz): δ [ppm] = 1.12-1.41 (m, 5 H), 1.64-1.92 (m, 5 H), 2.15 (s, 6 H), 3.70-3.83 (m, 1 H), 4.43 (s, 2 H), 4.98 (s, 2 H), 6.27-6.30 (m, 1 H), 6.90-6.93 (m, 3 H), 7.11-7.14 (m, 2 H), 7.36-7.43 (m, 5 H), 7.50-7.53 (m, 2 H), 8.64 (s, 1 H); ^{13}C-NMR ($CDCl_3$, 75 MHz): δ [ppm] = 15.4, 21.2, 21.4, 24.8, 25.6, 33.0, 48.5, 54.9, 66.0, 77.4, 78.5, 123.8, 126.7, 127.0, 128.3, 128.8, 128.9, 129.4, 129.6, 130.1, 131.5, 132.4, 134.5, 135.4, 137.9, 138.5, 147.2, 165.6, 167.7, 171.8.; HRMS calculated for $C_{31}H_{35}N_3O_4$: 514.2699 $[M+H]^+$, found 514.2700.

Compound **9b** (139 mg, 0.27 mmol, 1 eq.) was dissolved in methanol (20 mL) and a catalytical amount of Pd/C (10wt. %) was added. Subsequently, the mixture was stirred for 2 h at room temperature under a hydrogen atmosphere. Next, the solution was filtered over pad of Celite and the solvent was removed under reduced pressure. After purification by flash column chromatography (dichloromethane/methanol, gradient), the desired product **2b** was obtained in 54 % yield as pink solid: mp = 120 °C; ^{1}H-NMR (DMSO-d_6, 300 MHz): δ [ppm] = 1.00-1.34 (m, 5 H), 1.45-1.77 (m, 5 H), 2.13 (s, 6 H), 3.45-3.60 (m, 1 H), 4.37 (s, 2 H), 6.89-6.93 (m, 3 H), 7.19-7.21 (m, 2 H), 7.59-7.62 (m, 2 H), 7.84-7.94 (m, 1 H), 9.02 (s, 1 H), 11.19 (s, 1 H); ^{13}C-NMR (DMSO-d_6, 75 MHz): δ [ppm] = 20.7, 24.5, 25.2, 32.4, 47.8, 52.5, 59.1, 126.0, 126.8, 127.4, 130.1, 131.2, 135.8, 136.9, 146.4, 163.3, 166.7, 169.8; HRMS calculated for $C_{24}H_{29}N_3O_4$: 424.2231 $[M+H]^+$, found 424.2224; HPLC purity: 96.2 %.

General procedure A for the preparation of target compounds 2c-j via the Ugi-4CR:

Method 1: A mixture of methyl 4-(aminomethyl)benzoate hydrochloride (**6**) (1.2 eq.), the respective carbonyl (**4a-b**) (1.2 eq.), triethylamine (1.2 eq.) and crushed molecular sieves (MS, 4 Å, 50 mg for 0.5 mmol) in dry methanol (0.5 M) was added into a 10 mL glass pressure microwave tube equipped with a magnetic stirrer bar. The tube was closed with a silicon septum and the reaction mixture was subjected to microwave irradiation (Discover mode; power: 150 W; hold time: 30 min; temperature: 45 °C; PowerMax-cooling mode) under medium speed magnetic stirring. Next, the appropriate carboxylic acid (**5c, d-g**) (1.0 eq.) and isocyanide (**3a-c**) (1.0 eq.) components were added and the reaction mixture was again irradiated at 45 °C for 120 min (150W). Subsequently, after filtration of the molecular sieves, methanol (3 mL for 0.5 mmol) was added and the mixture was cooled to 0 °C. Then, aqueous hydroxylamine (50 %wt, ρ = 1.078 g/mL, 30 eq.) and sodium hydroxide (10 eq.) was added and the reaction mixture was stirred for 20 min at 0 °C. The solution was allowed to warm to room temperature and was stirred overnight. The solvent was evaporated under reduced pressure and the residue was dissolved in water (15 mL). The pH was adjusted to 7-8 using 1 M HCl and the formed solid was filtered, washed with water and diethyl ether to give the pure hydroxamic acid or was purified by flash column chromatography (dichloromethane/methanol, gradient) to yield the desired products **2c,e-h**.

Method 2: A mixture of methyl 4-(aminomethyl)benzoate hydrochloride (**6**) (1.2 eq.), the respective carbonyl (**4a, c**) (1.2 eq), triethylamine (1.2 eq.), and 50 mg (50 mg for 0.5 mmol) of crushed molecular sieves (MS) 4 Å in dry methanol (0.5 M) was added into a 10mL glass pressure microwave tube equipped with a magnetic stirrer bar. The tube was closed with a silicon septum and the reaction mixture was subjected to microwave irradiation (Discover mode; power: 150W; hold time: 20 min; temperature: 45 °C; PowerMax-cooling mode) under medium speed magnetic stirring. Next, the appropriate carboxylic acid (**5a-f**) (1.0 eq.) and isocyanide (**3a-c**) (1.0 eq.) components were added and the reaction mixture was again irradiated at 45 °C for 60 min (150W). Subsequently, a mixture of hydroxylamine hydrochloride (10 eq.) in a sodium methanolate solution, freshly prepared from dry methanol (8 mL) and sodium (7.5 mmol, 7.5 eq) was added and the reaction mixture was subjected to microwave irradiation at 55 °C for 30 min (150W). After completion of the reaction, the reaction mixture was filtered, and the solvent was removed under reduced pressure. Water (15 mL for 0.5 mmol) was added and the pH was adjusted to a pH 7-8 using 4 M HCl. The mixture was extracted with ethyl acetate, the combined organic layers were dried over anhydrous sodium sulfate, filtered, and concentrated in vacuum. The crude products were purified by flash column chromatography (dichloromethane/methanol, gradient) to yield the desired products **2d,i-j**.

***N*-(1-(Cyclohexylamino)-2-methyl-1-oxopropan-2-yl)-4-(dimethylamino)-*N*-(4-(hydroxycarbamoyl)benzyl)benzamide 2c:** Synthesized from **6**, cyclohexyl isocyanide (**3a**), acetone (**4b**), 4-(dimethylamino)benzoic acid (**5c**) according to the general procedure A (Method 1) in 88 % yield as a white solid: mp = 204-206 °C; ^{1}H-NMR (DMSO-d_6, 400 MHz): δ [ppm] = 1.03-1.24 (m, 5 H), 1.27 (s, 6 H), 1.53-1.66 (m, 5 H), 2.89 (s, 6 H), 3.41-3.54 (m, 1 H), 4.75 (s, 2 H), 6.62-6.64 (m, 2 H), 7.07-7.09 (m, 1 H), 7.38-7.41 (m, 4 H), 7.70-7.72 (m, 2 H), 9.01 (s, 1 H), 11.18 (s, 1 H); ^{13}C-NMR (DMSO-d_6, 101 MHz): δ [ppm] = 24.2, 24.9, 25.3, 32.4, 47.8, 50.1, 62.0, 111.0, 124.2, 126.7, 127.0, 128.2, 131.5, 143.3, 150.9, 163.9, 172.1, 173.0.; HRMS calculated for $C_{27}H_{36}N_4O_4$: 503.2629 $[M+Na]^+$, found 503.2630; HPLC purity: 97.5 %.

***rac*-*N*-(2-(Cyclohexylamino)-2-oxo-1-phenylethyl)-4-(dimethylamino)-*N*-(4-(hydroxycarbamoyl)benzyl)benzamide 2d:** Synthesized from **6**, cyclohexyl isocyanide (**3a**), benzaldehyde (**4c**), 4-(dimethylamino)benzoic acid (**5c**) according to the general procedure A (Method 2) in 56 % yield as a white solid: mp = 154 °C; ^{1}H-NMR (DMSO-d_6, 500 MHz): δ [ppm] = 0.97-1.37 (m, 5 H), 1.45-1.87 (m, 5 H), 2.94 (s, 6 H), 3.51-3.75 (m, 1 H), 4.23-4.52 (m, 1 H), 4.62-4.86 (m, 1 H), 5.77 (s, 1 H), 6.61-6.83 (m, 2 H), 6.93-7.42 (m, 9 H), 7.44-7.60 (m, 2 H), 7.91-8.07 (m, 1 H), 8.91 (s, 1 H), 11.05 (s, 1 H); ^{13}C-NMR (DMSO-d_6, 126 MHz): δ [ppm] = 24.3, 24.4, 25.1, 32.0, 39.6, 40.0, 47.6, 49.0, 64.0, 111.1, 122.7, 126.0, 126.4, 127.7, 128.2, 128.4, 128.6, 130.3, 136.5, 142.6, 151.2, 164.0, 168.1, 172.4; HRMS calculated for $C_{31}H_{36}N_4O_4$: 529.2809 $[M+H]^+$, found 529.2811; HPLC purity: 96.5 %.

***N*-(2-(*tert*-Butylamino)-2-oxoethyl)-*N*-(4-(hydroxycarbamoyl)benzyl)-2-methylbenzamide 2e:** Synthesized from **6**, *tert*-butyl isocyanide (**3b**), paraformaldehyde (**4a**), *o*-toluic acid (**5d**) according to the general procedure A (Method 1) in 11 % yield as a white solid: mp = 162-164 °C; ^{1}H-NMR (DMSO-d_6, 300 MHz): δ [ppm] = 1.15/1.26* (2 x s, 9 H), 2.23/2.33* (2 x s, 3 H), 3.43*/3.54 (2 x s, 2 H), 4.34/4.68 (s and brs, 2 H), 7.16-7.51 (m, 7 H), 7.65-7.83 (m, 2 H), 9.05 (brs, 1 H), 11.04 (brs, 1 H); ^{13}C-NMR (DMSO-d_6, 75 MHz): δ [ppm] = 18.6, 28.3, 28.6, 46.5, 48.3, 50.3, 50.7, 52.1, 125.5, 125.68, 125.73, 127.0, 127.15, 127.21, 127.8, 128.75, 128.78, 130.2, 130.3, 131.8, 132.0, 134.0, 134.3, 136.1, 136.1, 139.7, 140.7, 163.9, 166.6, 166.7, 171.1, 171.2; HRMS calculated for $C_{22}H_{27}N_3O_4$: 398.2074 $[M+H]^+$, found 398.2075; HPLC purity: 97.5 %.

***N*-(2-(*tert*-Butylamino)-2-oxoethyl)-*N*-(4-(hydroxycarbamoyl)benzyl)-2-methoxybenzamide 2f:** Synthesized from **6**, *tert*-butyl isocyanide (**3b**), paraformaldehyde (**4a**), 2-methoxybenzoic acid (**5e**) according to the general procedure A (Method 1) in 20 % yield as a white solid: mp = 139-141 °C; ^{1}H-NMR (DMSO-d_6, 400 MHz): δ [ppm] = 1.13/1.24* (2 x s, 9 H), 3.50-5.31 (m, 4 H), 3.74*/3.84 (2 x s, 3 H), 6.95-7.41 (m, 7 H), 7.69-7.78 (m, 2 H), 9.03 (brs, 1 H), 11.19 (brs, 1 H); ^{13}C-NMR (DMSO-d_6, 101 MHz): δ [ppm] = 28.4, 28.5, 47.2, 48.2, 50.1, 50.6, 52.4, 55.4, 55.6, 111.3, 111.6, 120.5, 120.7, 125.3, 125.6, 127.0, 127.1, 127.3, 127.6, 127.7, 130.3, 130.5, 131.5, 139.8, 140.6, 154.5, 154.8, 163.7, 163.8, 166.5, 166.7, 169.0,

169.2; HRMS calculated for $C_{22}H_{27}N_3O_5$: 414.2023 $[M+H]^+$, found 414.2025; HPLC purity: >99 %.

***N*-(2-(Benzylamino)-2-oxoethyl)-4-(*tert*-butyl)-*N*-(4-(hydroxycarbamoyl)benzyl)benzamide 2g:** Synthesized from **6**, benzyl isocyanide (**3c**), paraformaldehyde (**4a**), 4-*tert*-butylbenzoic acid (**5f**) according to the general procedure A (Method 1) in 38 % yield as a white solid: mp = 157-158 °C; ^{1}H-NMR (DMSO-d_6, 600 MHz): δ [ppm] = 1.26-1.29 (m, 9 H), 3.81/3.99* (2 x s, 2 H), 4.27/4.33* (2 x d, J = 5.4, 5.0 Hz, 2 H), 4.61*/4.68 (2 x s, 2 H), 7.20-7.21 (m, 1 H), 7.24-7.27 (m, 2 H), 7.32-7.33 (m, 3 H), 7.37-7.44 (m, 5 H), 7.74-7.76 (m, 2 H), 8.44-8.47 (m, 1 H) 9.41 (brs, 1 H), 10.38 (brs, 1 H); ^{13}C-NMR (DMSO-d_6, 126 MHz): δ [ppm] = 30.9, 34.4, 42.1, 47.5, 48.7, 51.1, 53.1, 125.0, 126.4, 126.7, 127.0, 127.2, 127.5, 128.1, 131.7, 131.9, 132.8, 133.0, 139.0, 139.2, 139.9, 140.3, 152.1, 163.8, 167.7, 171.3; HRMS calculated for $C_{28}H_{31}N_3O_4$: 474.2387 $[M+H]^+$, found 474.2390; HPLC purity: 98.1 %.

***N*-(2-(Benzylamino)-2-oxoethyl)-*N*-(4-(hydroxycarbamoyl)benzyl)-4-isopropylbenzamide 2h:** Synthesized from **6**, benzyl isocyanide (**3c**), paraformaldehyde (**4a**), 4-*i*-propylbenzoic acid (**5a**) according to the general procedure A (Method 1) in 45 % yield as a white solid: mp = 189-190 °C; ^{1}H-NMR (DMSO-d_6, 400 MHz): δ [ppm] = 1.18-1.22 (m, 6 H), 2.85-2.95 (m, 1 H), 3.81/3.99* (2 x s, 2 H), 4.27-4.33 (m, 2 H), 4.60*/4.68 (2 x s, 2 H), 7.18-7.40 (12 H), 7.74-7.76 (m, 1 H), 8.43-8.44 (m, 1 H), 9.03 (s, 1 H), 11.21 (s, 1 H); ^{13}C-NMR (DMSO-d_6, 101 MHz): δ [ppm] = 23.7, 33.3, 42.1, 42.2, 47.6, 48.8, 51.1, 53.2, 126.3, 126.8, 126.9, 127.1, 127.3, 127.7, 128.3, 131.7, 131.9, 133.2, 133.5, 139.0, 139.3, 140.2, 140.5, 150.0, 150.2, 163.9, 164.0, 167.7, 167.9, 171.5; HRMS calculated for $C_{27}H_{29}N_3O_4$: 460.2231 $[M+H]^+$, found 460.2234; HPLC purity: >99 %.

***N*-(2-(Benzylamino)-2-oxoethyl)-4-(dimethylamino)-*N*-(4-(hydroxycarbamoyl)benzyl)benzamide 2i:** Synthesized from **6**, benzyl isocyanide (**3c**), paraformaldehyde (**4a**), 4-(dimethylamino)benzoic acid (**5c**) according to the general procedure A (Method 2) in 83 % yield as a white solid: mp = 193 °C; ^{1}H-NMR (DMSO-d_6, 300 MHz): δ [ppm] = 2.93 (s, 6 H), 3.90 (s, 2 H), 4.30 (d, J = 5.8 Hz, 2 H), 4.67 (s, 2 H), 6.55-6.75 (m, 2 H), 7.14-7.46 (m, 9 H), 7.66-7.83 (m, 2 H), 8.32-8.60 (m, 1 H), 9.03 (s, 1 H), 11.20 (s, 1 H); ^{13}C-NMR (DMSO-d_6, 75 MHz): δ [ppm] = 39.7, 42.1, 111.0, 121.9, 126.86, 126.92, 127.0, 127.2, 127.3, 128.3, 128.6, 131.7, 139.2, 140.8, 151.2, 164.0, 168.15, 171.7; HRMS calculated for $C_{26}H_{28}N_4O_4$: 461.2183 $[M+H]^+$, found 461.2182; HPLC purity: 98.2 %.

***N*-(2-(Benzylamino)-2-oxoethyl)-*N*-(4-(hydroxycarbamoyl)benzyl)-3,5-dimethylbenzamide 2j:** Synthesized from **6**, benzyl isocyanide (**3c**), paraformaldehyde (**4a**), 3,5-dimethylbenzoic acid (**5b**) according to the general procedure A (Method 2) in 77 % yield as a white solid: mp = 194 °C; ^{1}H-NMR (DMSO-d_6, 300 MHz): δ [ppm] = 2.24 (s, 6 H), 3.79/3.99* (2 x s, 2 H), 4.21-4.41 (m, 2 H), 4.55*/4.68 (2 x s, 2 H), 6.96-7.13 (m, 3 H), 7.12-7.48 (m, 7 H), 7.69-7.87 (m, 2 H), 8.33-8.52 (m ,1 H), 9.03 (s, 1 H), 11.21 (s, 1 H); ^{13}C-NMR (DMSO-d_6, 126 MHz): δ [ppm] = 20.7, 42.1, 47.4, 48.6, 51.0, 53.1, 124.0, 126.8, 127.1, 127.6, 128.2, 130.7, 131.7, 135.9, 137.5, 139.0, 140.4, 163.95, 167.7, 171.5; HRMS calculated for $C_{26}H_{27}N_3O_4$: 446.2074 $[M+H]^+$, found 446.2077; HPLC purity: >99 %.

General Procedure B for the synthesis of intermediates 12k-r (submonomer pathway 1): To a solution of methyl-4-(aminomethyl)benzoate hydrochloride (**6**) (5.000 g, 0.025 mol, 1 eq.) in THF (50 mL) was added triethylamine (10.31 mL, 0.075 mol, 3 eq.), followed by the addition of *tert*-butyl-bromoacetate (4.40 mL, 0.030, 1.2 eq.). The suspension was stirred over night at room temperature. Further *tert*-butyl-bromoacetate (0.74 mL, 0.005 mol, 0.2 eq.) was added, because of incomplete consumption of the starting material and the solution was stirred at room temperature for additional 4 h. After filtration, the solvent was evaporated, and the residue was dissolved in ethyl acetate (75 mL) and washed with water (2 x 30 mL). The organic layer was dried over Na_2SO_4 and the solvent was removed under reduced pressure. Column chromatographic purification (*n*-hexane/EtOAc, gradient) afforded product **10** in 46 % yield as a yellowish wax (3.191 g). ^{1}H-NMR ($CDCl_3$, 600 MHz): δ [ppm] = 1.47 (s, 9 H), 1.82 (brs, 1 H), 3.30 (s, 2 H), 3.85 (s, 2 H), 3.91 (s, 3 H), 7.40-7.42 (m, 2 H), 7.98-8.01 (m, 2 H); ^{13}C-NMR ($CDCl_3$, 151 MHz): δ [ppm] = 28.3, 51.1, 52.2, 53.1, 81.5, 128.2, 129.2, 129.9, 145.2, 167.2, 171.7; Elemental analysis calculated for $C_{15}H_{21}NO_4$: C 64.50, H 7.58, N 5.01, found: C 64.66, H 7.51, N 5.07.

To a solution of **10** (2.700 g, 0.0097 mol, 0.01 eq.) and Et_3N (1.68 mL, 0.012 mol, 1.25 eq.) in dichloromethane (50 mL) was added 3,5-dimethylbenzoyl chloride (1.57 mL, 0.011 mol, 1.1 eq.). The mixture was stirred over night at room temperature. The reaction was quenched with water (175 mL) and diluted with dichloromethane (200 mL). The organic layer was washed with a HCl-solution (1 M, 100 mL) and dried over Na_2SO_4. After filtration and removal of the solvent under reduced pressure, column chromatographic purification (*n*-hexane/EtOAc = gradient) afforded the desired product **11** in 99 % yield as a white wax (3.919 g): ^{1}H-NMR ($CDCl_3$, 600 MHz): δ [ppm] = 1.43*/1.49 (2 x s, 9 H), 2.28*/2.31 (2 x s, 6 H), 3.92-3.93 (m, 3 H), 3.75*/4.04 (2 x s, 2 H), 4.64/4.85* (s, 2 H), 7.03-7.08 (m, 3 H), 7.26-7.27 (m, 1 H), 7.40-7.41 (m, 1 H) 8.02-8.03 (m, 2 H); ^{13}C-NMR ($CDCl_3$, 151 MHz): δ [ppm] = 21.4, 28.1, 28.3, 47.2, 49.2, 51.0, 52.29, 52.35, 53.7, 82.2, 82.5, 124.3, 124.5, 127.1, 128.5, 129.7 , 129.9, 130.2, 130.3, 131.6, 131.7, 135.4, 135.7, 142.0, 142.1, 166.8, 167.0, 168.1, 168.5, 172.9, 173.1; Elemental analysis calculated for $C_{24}H_{29}NO_5$: C 70.05, H 7.10, N 3.40, found: C 70.04, H 7.36, N 3.29.

Compound **11** (731 mg, 1.78 mmol, 1 eq.) was stirred in trifluoroacetic acid/dichloromethane (1:1, 10 mL) at room temperature until complete consumption of the starting material. Afterwards, the solvent was evaporated under reduced pressure. Further trifluoroacetic acid was subsequently removed by codestillation with toluene, which afforded the corresponding *N*-(3,5-dimethylbenzoyl)-*N*-(4-(methoxycarbonyl)benzyl)-glycine in >99 % yield as a yellow solid (664 mg): mp = 141-146 °C; ^{1}H-NMR (300 MHz, DMSO-d_6): δ [ppm] = 2.21-2.32 (m, 6 H), 3.85 (s, 3 H), 3.89*/4.02 (2 x s, 2 H), 4.58*/4.73 (2 x s, 2 H), 6.94-7.25 (m, 3 H), 7.36-7.64 (m, 2 H), 7.91-8.04 (m, 2 H), 12.82 (brs, 1 H); ^{13}C NMR (151 MHz, DMSO-d_6): δ [ppm] = 20.72, 20.75, 20.8, 46.7, 47.1, 48.9, 49.5, 50.7, 52.11, 52.12, 52.3, 53.1, 123.9, 124.0, 126.4, 127.0, 127.2, 127.9, 128.5, 128.7, 129.4, 129.46, 129.49, 130.4, 130.7, 131.0, 131.1, 134.2, 135.5, 135.8, 136.7, 137.7, 137.8, 142.8, 143.0, 165.8, 166.0, 166.1, 167.5, 168.0, 170.1, 170.7, 171.6.; HRMS calculated for $C_{20}H_{21}NO_5$: 356.1492 $[M+H]^+$, found 356.1493.

To a solution of *N*-(3,5-dimethylbenzoyl)-*N*-(4-(methoxycarbonyl)benzyl)-glycine (1 eq.), EDC hydrochloride (1.2 eq.) and DMAP (0.3 eq.) in dichloromethane (5 mL for 0.5 mmol) was added the appropriate amine (1 eq.). The mixture was stirred over night at room temperature. The solution was diluted with dichloromethane (25 mL) and washed with distilled water (15 mL) and 1 N HCl-solution (2 x 15 mL). The organic layer was dried over $MgSO_4$ and the solvent was evaporated under reduced pressure. The residue was purified by column chromatography (*n*-hexane/ethyl acetate, gradient) or by recrystallization (ethyl acetate/n-hexane) to give the desired products **12k-r**.

Methyl 4-((*N*-(2-((3,5-dimethylbenzyl)amino)-2-oxoethyl)-4-methylbenzamido)methyl)-benzoate 12k: The compound was obtained as described in the general procedure B using 4-methylbenzylamine in 80 % yield as a white solid: mp = 160-168 °C; ^{1}H-NMR ($CDCl_3$, 300 MHz): δ [ppm] = 2.26 (s, 6 H), 2.33 (s, 3 H), 3.83*/4.07 (2 x s, 2 H), 3.92 (s, 3 H), 4.36-4.41 (m, 2 H), 4.69/4.82* (2 x s, 2 H), 6.12-6.19*/6.76 (m and brs, 1 H), 6.98-7.03 (m, 3 H), 7.08-7.15 (m, 4 H) 7.23-7.36 (m, 2 H), 7.99-8.02 (m, 2 H); ^{13}C-NMR ($CDCl_3$, 151 MHz): δ [ppm] = 21.2, 21.3, 43.4, 49.5, 52.3, 54.0, 124.4, 127.2, 127.8, 128.0, 129.5, 129.8, 130.3, 132.0, 134.9, 135.2, 137.3, 138.5, 141.5, 141.8, 166.8, 168.5, 173.6; HRMS calculated for $C_{28}H_{30}N_2O_4$: 459.2278 $[M+H]^+$, found 459.2284.

Methyl 4-((*N*-(2-((4-methoxybenzyl)amino)-2-oxoethyl)-3,5-dimethylbenzamido)methyl)-benzoate 12l: The compound was obtained as described in the general procedure B from 4-methoxybenzylamine in 82 % yield as a yellowish solid: mp = 154-161 °C;

^{1}H-NMR ($CDCl_3$, 600 MHz): δ [ppm] = 2.25 (s, 6 H), 3.79 (s, 3 H), 3.82*/4.06 (2 x s, 2 H), 3.91 (s, 3 H), 4.33-4.36 (m, 2 H), 4.69/4.82* (2 x s, 2 H), 6.14*/6.73 (2 x s, 1 H), 6.85-6.86 (m, 2 H), 6.98-7.03 (m, 3 H), 7.13-7.24 (m, 3 H), 7.31-7.41 (m, 1 H), 7.99-8.01 (m, 2 H); ^{13}C-NMR ($CDCl_3$, 151 MHz): δ [ppm] = 21.3, 43.1, 49.5, 52.3, 54.1, 55.4, 114.2, 124.4, 127.2, 128.4, 129.1, 129.4, 129.9, 130.2, 134.9, 138.6, 141.5, 159.1, 166.8, 166.8, 168.4, 173.5; HRMS calculated for $C_{28}H_{30}N_2O_5$: 475.2227 $[M+H]^+$, found 475.2227.

Methyl 4-((*N*-(2-((4-fluorobenzyl)amino)-2-oxoethyl)-3,5-dimethylbenzamido)methyl)benzoate 12m: The compound was obtained as described in the general procedure B using 4-fluorobenzylamine in 62 % yield as a white solid: mp = 182-184 °C; ^{1}H-NMR ($CDCl_3$, 600 MHz): δ [ppm] = 2.29 (s, 6 H), 3.87*/4.10 (2 x s, 2 H), 3.95 (s, 3 H), 4.39-4.42 (m, 2 H), 4.72-4.85 (m, 2 H), 6.20-6.25*/6.87 (m and s, 1 H), 7.00-7.39 (m, 9 H), 8.03-8.04 (m, 2 H); ^{13}C-NMR ($CDCl_3$, 126 MHz): δ [ppm] = 21.3, 43.0, 49.8, 52.3, 54.2, 76.9, 77.2, 77.4, 115.6, 115.8, 124.5, 127.3, 129.5, 130.0, 130.3, 132.0, 134.1, 135.0, 138.6, 141.5, 161.4, 163.4, 166.7, 168.6, 173.6; HRMS calculated for $C_{27}H_{27}FN_2O_4$: 463.2028 $[M+H]^+$, found 463.2032.

Methyl 4-((*N*-(2-((4-chlorobenzyl)amino)-2-oxoethyl)-3,5-dimethylbenzamido)methyl)-benzoate 12n: The compound was obtained as described in the general procedure B using 4-chlorobenzylamine in 66 % yield as a white solid: mp = 177-180 °C; ^{1}H-NMR ($CDCl_3$, 300 MHz): δ [ppm] = 2.27 (s, 6 H), 3.86-4.08 (m, 2 H), 3.93 (s, 3 H), 4.39-4.41 (m, 2 H), 4.70-4.85 (m, 2 H), 6.05*/6.87 (brs and s, 1 H), 6.98-7.05 (m, 3 H), 7.12-7.24 (m, 3 H), 7.28-7.42 (m, 3 H), 8.00-8.03 (m, 2 H); ^{13}C-NMR ($CDCl_3$, 126 MHz): δ [ppm] = 21.3, 35.8, 42.9, 49.8, 52.3, 54.3, 77.1, 77.2, 77.36, 77.41, 124.4, 127.3, 129.0, 129.2, 130.0, 130.3, 132.0, 133.5, 134.9, 136.9, 138.6, 141.5, 166.7, 168.6, 173.6; HRMS calculated for $C_{27}H_{27}ClN_2O_4$: 479.1732 $[M+H]^+$, found 479.1735.

Methyl 4-((*N*-(2-((4-(*tert*-butyl)benzyl)amino)-2-oxoethyl)-3,5-dimethylbenzamido)methyl)benzoate 12o: The compound was obtained as described in the general procedure B using 4-*tert*-butylbenzylamine in 57 % yield as a white solid: mp = 99-100 °C; ^{1}H-NMR ($CDCl_3$, 600 MHz): δ [ppm] = 1.34 (s, 9 H), 2.29 (s, 6 H), 3.86*/4.11 (2 x s, 2 H), 3.95 (s, 3 H), 4.40-4.45 (m, 2 H), 4.74/4.88* (2 x s, 2 H), 6.00*/6.71 (2 x s, 1 H), 7.04-7.06 (m, 3 H), 7.19-7.39 (m, 6 H), 8.03-8.05 (m, 2 H); ^{13}C-NMR ($CDCl_3$, 126 MHz): δ [ppm] = 21.34, 31.49, 34.69, 43.40, 49.70, 52.27, 54.14, 76.90, 77.16, 77.41, 124.51, 125.84, 127.26, 127.58, 128.46, 130.00, 130.31, 131.95, 135.08, 138.59, 141.66, 150.73, 166.77, 168.47, 173.52; HRMS calculated for $C_{31}H_{36}N_2O_4$: 501.2748 $[M+H]^+$, found 501.2752.

Methyl 4-((*N*-(2-((3,5-dimethylbenzyl)amino)-2-oxoethyl)-3,5-dimethylbenzamido)-methyl)benzoate 12p: The compound was obtained as described in the general procedure B using 3,5-dimethylbenzylamine in 56 % yield as a white solid: mp = 177-181 °C; ^{1}H-NMR ($CDCl_3$, 600 MHz): δ [ppm] = 2.26*/2.29 (2 x s, 12 H), 3.83*/4.09 (2 x s, 2 H), 3.92 (s, 3 H), 4.32-4.36 (m, 2 H), 4.71/4.84* (2 x s, 2 H), 6.01*/6.76 (2 x s, 1 H), 6.83-7.03 (m, 6 H), 7.23-7.37 (m, 2 H), 8.00-8.01 (m, 2 H); ^{13}C-NMR ($CDCl_3$, 151 MHz): δ [ppm] = 21.3, 21.4, 43.5, 49.5, 52.3, 54.0, 124.4, 125.5, 127.1, 128.5, 129.2, 129.9, 132.0, 134.9, 138.0, 138.4, 138.5, 141.5, 166.8, 168.5, 173.6; HRMS calculated for $C_{29}H_{32}N_2O_4$: 473.2435 $[M+H]^+$, found 473.2437.

Methyl 4-((3,5-dimethyl-*N*-(2-((3-methylbenzyl)amino)-2-oxoethyl)benzamido)methyl)benzoate 12q: The compound was obtained as described in the general procedure B using 3-methylbenzylamine in 63 % yield as a white solid: mp = 156-158 °C; ^{1}H-NMR ($CDCl_3$, 600 MHz): δ [ppm] = 2.29 (s, 6 H), 2.36 (s, 3 H), 3.86*/4.11 (2 x s, 2 H), 3.94 (s, 3 H), 4.40-4.44 (m, 2 H), 4.73/4.88* (2 x s, 2 H), 5.92-6.00*/6.79 (m and s, 1 H), 6.99-7.41 (m, 9 H), 8.03-8.04 (m, 2 H); ^{13}C-NMR ($CDCl_3$, 126 MHz): δ [ppm] = 21.3, 21.5, 43.7, 49.7, 52.3, 54.1, 124.5, 124.9, 127.2, 128.4, 128.6, 128.8, 130.0, 130.3, 132.0, 135.0, 138.2, 138.6, 141.6, 166.8, 168.5, 173.5; HRMS calculated for $C_{28}H_{30}N_2O_4$: 459.2278 $[M+H]^+$, found 459.2282.

Methy 4-((3,5-dimethyl-*N*-(2-oxo-2-((pyridin-3-ylmethyl)amino)ethyl)benzamido)methyl)-benzoate 12r: The compound was obtained as described in the general procedure B using 3-picolylamine in 77 % yield as a white solid: mp = 175-178 °C; ^{1}H-NMR ($CDCl_3$, 300 MHz): δ [ppm] = 2.26 (s, 6 H), 3.85*/4.08 (2 x s, 2 H), 3.92 (s, 3 H), 4.43-4.45 (m, 2 H), 4.70-4.83 (m, 2 H), 6.51-7.04 (m, 4 H), 7.23-7.25 (m, 2 H), 7.31-7.62 (m, 2 H), 7.99-8.02 (m, 2 H,), 8.51-8.53 (m, 2 H); ^{13}C-NMR ($CDCl_3$, 126 MHz): δ [ppm] = 21.3, 41.1, 43.1, 49.6, 52.3, 54.3, 77.2, 123.7, 124.5, 124.9, 126.6, 127.2, 128.5, 130.1, 130.3, 132.1, 133.4, 134.0, 134.9, 135.6, 138.6, 141.5, 149.0, 149.3, 166.7, 168.9, 173.7; HRMS calculated for $C_{26}H_{27}N_3O_4$: 446.2074 $[M+H]^+$, found 446.2075.

General Procedure C for the synthesis of intermediates 15s-t (submonomer pathyway 2): A mixture of methylamine hydrochloride (1.674 g, 0.025 mol, 1 eq.) and K_2CO_3 (6.855 g, 0.050 mol, 2 eq.) in dichloromethane (75 mL) was cooled to 0 °C under nitrogen atmosphere. Bromoacetyl bromide (2.15 mL, 0.025 mol, 1 eq.) was then added dropwise under vigorous stirring. The solution was stirred for 1 h at 0 °C followed by 2 h at room temperature. Subsequently, water (25 mL) was added to the solution followed by phase separation and drying of the organic phase over Na_2SO_4 overnight. After filtration, the solvent was removed under reduced pressure and 2-bromo-*N*-methylacetamide (**CAUTION**: This substance is an irritant and must be handled with care) was obtained as a white solid (1.730 g) in 46 % yield: ^{1}H-NMR ($CDCl_3$, 300 MHz): δ [ppm] = 2.85 (d, 3 H), 3.87 (s, 2 H), 6.60 (brs, 1 H); ^{13}C-NMR $CDCl_3$, 75 MHz): δ [ppm] = 27.1, 29.3, 166.1.

To a solution of methyl 4-(aminomethyl)benzoate hydrochloride (**6**) (2.335 g, 0.012 mol, 1.1 eq.) and triethylamine (4.52 mL, 0.033 mol, 3.1 eq.) in THF (20 mL) was added 2-bromo-*N*-methylacetamide (1.600 g, 0.011 mol, 1 eq.) in three portions. The mixture was then stirred at room temperature overnight. The mixture was filtered, and the solvent was removed under reduced pressure. The residue was dissolved in ethyl acetate (50 mL), washed with water (2 x 20 mL), dried over Na_2SO_4 and the solvent was removed under reduced pressure. The product (**14**) was obtained after flash column chromatography (*n*-hexane/ethyl acetate, gradient) as a white solid in 50 % yield (1.235 g): mp = 76-78 °C; ^{1}H-NMR (DMSO-d_6, 600 MHz): δ [ppm] = 2.60 (d, J = 4.7 Hz, 3 H), 2.71 (brs, 1 H), 3.05 (s, 2 H), 3.74 (s, 2 H), 3.84 (s, 3 H), 7.48-7.50 (m, 2 H,), 7.76-7.77 (m, 1 H), 7.90-7.91 (m, 2 H); ^{13}C-NMR (DMSO-d_6, 125 MHz): δ [ppm] = 25.2, 51.4, 51.9, 52.3, 128.0, 128.0, 128.8, 129.0, 146.2, 166.1, 171.2; HRMS calculated for $C_{12}H_{16}N_2O_3$: 237.1234 $[M+H]^+$, found 237.1237.

The amine (**14**) (1 eq.) was dissolved in dichloromethane (5 mL for 1.1 mmol amine) followed by the addition of triethylamine (1.25 eq.). Subsequently, the respective acyl chloride (1.1 eq.) was added and the solution was stirred at room temperature overnight. The reaction mixture was quenched by the addition of water (15 mL) followed by dilution with dichloromethane (25 mL). The organic phase was separated, washed with 1 M HCl (15 mL) and dried over Na_2SO_4. After filtration the solvent was evaporated under reduced pressure and the residue was purified either by recrystallization from dichloromethane and *n*-hexane or by flash column chromatography (*n*-hexane/ethylacetate, gradient) to give the respective ester (**15s-t**).

Methyl 4-((3,5-dimethyl-*N*-(2-(methylamino)-2-oxoethyl)benzamido)methyl)benzoate 15s: The compound was obtained as described in the general procedure C using 3,5-dimethylbenzoyl chloride in 88 % yield as a white solid: mp = 218-219 °C; ^{1}H-NMR ($CDCl_3$, 600 MHz): δ [ppm] = 2.27-2.30 (m, 6 H), 2.80 (s, 3 H), 3.80*/4.04 (2 x s, 2 H), 3.92 (s, 3 H), 4.70/4.84* (2 x s, 2 H), 5.79*/6.43 (2 x s, 1 H), 7.03-7.05 (m, 3 H), 7.24-7.40 (m, 2 H), 8.02-8.03 (m, 2 H); ^{13}C-NMR ($CDCl_3$, 151 MHz): δ [ppm] = 21.4, 26.4, 49.6, 52.3, 54.2, 124.4, 124.6, 127.2, 128.5, 129.9, 130.3, 132.1, 134.8, 138.6, 141.6, 166.8, 169.4,

173.6; HRMS calculated for $C_{21}H_{24}N_2O_4$: 369.1809 $[M+H]^+$, found 369.1815.

Methyl 4-((2-methyl-*N*-(2-(methylamino)-2-oxoethyl)benzamido)methyl)benzoate 15t: The compound was obtained as described in the general procedure C using 2-methylbenzoyl chloride in 46 % yield as a white solid: mp = 92-94 °C; ^{1}H-NMR ($CDCl_3$, 300 MHz): δ [ppm] = 2.30*/2.36 (2 x s, 3 H), 2.73*/2.84 (2 x d, J = 4.8, 4.9 Hz, 3 H), 3.62-4.09 (m, 2 H), 3.91/3.92* (2 x s, 3 H), 4.55/4.90* (s and brs, 2 H), 5.44*/6.26 (2 x s, 1 H), 7.15-7.46 (m, 6 H), 7.97-8.05 (m, 2 H); ^{13}C-NMR ($CDCl_3$, 75 MHz): δ [ppm] = 19.1, 19.2, 26.3, 43.7, 46.0, 48.4, 48.6, 51.1, 52.3, 53.3, 125.7, 125.8, 126.0, 126.1, 126.8, 127.5, 127.7, 128.7, 129.5, 129.6, 129.7, 129.99, 130.08, 130.2, 130.3, 130.9, 131.3, 134.6, 134.9, 135.1, 141.1, 141.9, 166.7, 168.2, 169.1, 173.1.; HRMS calculated for $C_{20}H_{22}N_2O_4$: 355.1652 $[M+H]^+$, found 355.1656.

General procedure D for the preparation of hydroxamic acids synthesized by the submonomer pathways (2k-t): The appropriate ester (1 eq.) was dissolved in dichloromethane/methanol (1:3, 6 mL for 0.3 mmol) and the solution was cooled to 0 °C. This was followed by the addition of aq. hydroxylamine solution (50 %wt, 30 eq.) and sodium hydroxide (10 eq.). The mixture was allowed to warm to room temperature and was stirred overnight. Next, the solvent was removed under reduced pressure. The residue was dissolved in distilled water (20 mL) and the solution was acidified with 1 M HCl-solution to pH 7-8. The precipitate was washed with diethyl ether several times, recrystallized from dichloromethane and diethyl ether or purified by column chromatography (dichloromethane/methanol, gradient) to give the desired product. In some cases, the respective carboxylic acid has formed as a side product, which was removed by using the anion exchange sorbent Isolute PE-AX® (with methanol as the eluent).

***N*-(4-(Hydroxycarbamoyl)benzyl)-3,5-dimethyl-*N*-(2-((4-methylbenzyl)amino)-2-oxoethyl)benzamide 2k:** The hydroxamic acid was obtained as described in the general procedure D using ester **12k** in 82 % yield as a white solid: mp = 147-149 °C; ^{1}H-NMR (DMSO-d_6, 300 MHz): δ [ppm] = 2.24 (s, 6 H), 2.27 (s, 3 H), 3.77/3.97* (2 x s, 2 H), 4.21/4.26* (2 x d, J = 5.6, 5.7 Hz, 2 H), 4.54*/4.67 (2 x s, 2 H); 7.02-7.40 (m, 9 H), 7.73-7.87 (m, 2 H), 8.35-8.41 (m, 1 H), 9.16 (brs, 1 H), 11.24 (brs, 1 H); ^{13}C-NMR (DMSO-d_6, 126 MHz): δ [ppm] = 20.5, 20.7, 41.9, 47.4, 48.6, 51.0, 53.1, 124.0, 125.9, 126.8, 127.1, 127.6, 128.7, 129.3, 130.7, 131.7, 135.9, 136.1, 137.5, 140.3, 163.8, 167.6, 171.5; HRMS calculated for $C_{27}H_{29}N_3O_4$: 460.2231 $[M+H]^+$, found 460.2237; HPLC purity: 95.4 %.

***N*-(4-(Hydroxycarbamoyl)benzyl)-*N*-(2-((4-methoxybenzyl)amino)-2-oxoethyl)-3,5-dimethylbenzamide 2l:** The hydroxamic acid was obtained as described in the general procedure D using ester **12l** in 38 % yield as a white solid: mp = 123-130 °C ^{1}H-NMR (DMSO-d_6, 300 MHz): δ [ppm] = 2.22 (s, 6 H), 3.70 (s, 3 H), 3.72/3.93* (2 x s, 2 H), 4.16-4.22 (m, 2 H), 4.50*/4.63 (2 x s, 2 H), 6.83-6.85 (m, 2 H), 6.99-7.33 (m, 7 H), 7.70-7.72 (m, 2 H), 8.30-8.37 (m, 1 H); ^{13}C-NMR (DMSO-d_6, 101 MHz): δ [ppm] = 20.8, 25.0, 41.6, 41.6, 47.2, 48.5, 50.8, 53.2, 55.1, 113.7, 124.1, 126.6, 126.7, 127.5, 128.5, 128.6, 130.8, 131.1, 131.2, 133.5, 133.9, 135.9, 136.1, 137.56, 137.59, 138.6, 139.0, 158.2, 158.3, 162.9, 163.0, 167.5, 167.6, 171.5, 175.0; HRMS calculated for $C_{27}H_{29}N_3O_5$: 476.2180 $[M+H]^+$, found 476.2182; HPLC purity: 95.6 %.

***N*-(2-((4-Fluorobenzyl)amino)-2-oxoethyl)-*N*-(4-(hydroxycarbamoyl)benzyl)-3,5-dimethylbenzamide 2m:** The hydroxamic acid was obtained as described in the general procedure D using ester **12m** in 91 % yield as a white solid: mp = 185-187 °C; ^{1}H-NMR (DMSO-d_6, 600 MHz): δ [ppm] = 2.23 (s, 6 H), 3.79/3.98* (2 x s, 2 H), 4.25/4.30* (2 x d, J = 5.7, 5.5 Hz, 2 H), 4.55*/4.68 (2 x s, 2 H), 7.01-7.08 (m, 3 H), 7.12-7.16 (m, 2 H), 7.21-7.35 (m, 3 H), 7.38-7.40 (m, 1 H), 7.74-7.92 (m, 2 H), 8.43-8.47 (m, 1 H), 9.10 (brs, 1 H), 11.23 (brs, 1 H); ^{13}C-NMR (DMSO-d_6, 126 MHz): δ [ppm] = 20.6, 41.4, 47.5, 48.6, 51.0, 53.1, 114.8, 114.9, 124.0, 126.8, 127.0, 127.6, 129.0, 129.1, 129.2, 129.4, 130.7, 131.7, 131.8, 135.2, 135.4, 135.8, 135.9, 137.5, 140.1, 140.3, 160.2, 162.1, 163.8, 167.7, 171.48, 171.48; HRMS calculated for $C_{26}H_{26}FN_3O_4$: 464.1980 $[M+H]^+$, found 464.1981; HPLC purity: 95.1 %.

***N*-(2-((4-Chlorobenzyl)amino)-2-oxoethyl)-*N*-(4-(hydroxycarbamoyl)benzyl)-3,5-dimethylbenzamide 2n:** The hydroxamic acid was obtained as described in the general procedure D using ester **12n** in 70 % yield as a white solid: mp = 149-150 °C; ^{1}H-NMR (DMSO-d_6, 300 MHz): δ [ppm] = 2.23 (s, 6 H), 3.79/3.98* (2 x s, 2 H), 4.24/4.29* (2 x d, J = 5.6, 5.7 Hz, 2 H), 4.55*/4.67 (2 x s, 2 H), 7.00-7.07 (m, 3 H), 7.18-7.45 (m, 6 H), 7.73-7.94 (m, 2 H), 8.42-8.49 (m, 1 H), 9.04 (s, 1 H), 11.22 (s, 1 H); ^{13}C-NMR (DMSO-d_6, 126 MHz): δ [ppm] = 20.6, 41.4, 47.4, 48.6, 50.9, 53.1, 124.0, 125.7, 126.6, 126.9, 127.4, 128.1, 128.9, 129.0, 129.21, 130.7, 131.3, 131.8, 132.4, 135.9, 137.4, 138.1, 139.3, 139.7, 163.7, 167.8, 171.5; HRMS calculated for $C_{26}H_{26}ClN_3O_4$: 480.1685 $[M+H]^+$, found 480.1687; HPLC purity: 98.0 %.

***N*-(2-((4-(*tert*-Butyl)benzyl)amino)-2-oxoethyl)-*N*-(4-(hydroxycarbamoyl)benzyl)-3,5-dimethylbenzamide 2o:** The hydroxamic acid was obtained as described in the general procedure D using ester **12o** in 80 % yield as a reddish solid: mp = 180-183 °C; ^{1}H-NMR (DMSO-d_6, 600 MHz): δ [ppm] = 1.26 (s, 9 H), 2.23 (s, 6 H), 3.77/3.97* (2 x s, 2 H), 4.22/4.28* (2 x d, J = 5.5, 5.2 Hz, 2 H), 4.55*/4.68 (2 x s, 2 H), 7.01-7.07 (m, 3 H), 7.10-7.19 (m, 2 H), 7.27-7.40 (m, 4 H), 7.74-7.89 (m, 2 H), 8.39-8.36 (m, 1 H), 9.05 (brs, 1 H), 11.17 (brs, 1 H); ^{13}C-NMR (DMSO-d_6, 126 MHz): δ [ppm] = 20.6, 31.0, 34.0, 41.8, 47.4, 48.6, 50.9, 53.1, 124.0, 124.9, 126.8, 127.0, 127.5, 130.7, 131.7, 131.8, 135.9, 136.1, 137.4, 140.3, 149.2, 163.8, 167.6, 171.5; HRMS calculated for $C_{30}H_{35}N_3O_4$: 502.2700 $[M+H]^+$, found 502.2701; HPLC purity: 95.3 %.

***N*-(2-((3,5-Dimethylbenzyl)amino)-2-oxoethyl)-*N*-(4-(hydroxycarbamoyl)benzyl)-3,5-dimethylbenzamide 2p:** The hydroxamic acid was obtained as described in the general procedure D using ester **12p** in 58 % yield as a white solid: mp = 116-118 °C; ^{1}H-NMR (DMSO-d_6, 300 MHz): δ [ppm] = 2.23 (s, 12 H), 3.77/3.97* (2 x s, 2 H), 4.19/4.25* (2 x d, J = 5.5, 5.3 Hz, 2 H), 4.55*/4.67 (2 x s, 2 H), 6.80-6.87 (m, 3 H), 7.02-7.06 (m, 3 H), 7.25-7.39 (m, 2 H), 7.73-7.76 (m, 2 H), 8.29-8.41 (m, 1 H), 10.14 (brs, 1 H); ^{13}C-NMR (DMSO-d_6, 126 MHz): δ [ppm] = 20.6, 20.8, 42.1, 47.2, 48.4, 50.7, 53.1, 113.9, 124.1, 124.9, 125.0, 126.5, 126.7, 127.3, 128.2, 129.0, 129.2, 130.7, 133.5, 136.0, 137.1, 137.4, 138.9, 163.6, 167.5, 171.4; HRMS calculated for $C_{28}H_{31}N_3O_4$: 474.2387 $[M+H]^+$, found 474.2391; HPLC purity: 97.1 %.

***N*-(4-(Hydroxycarbamoyl)benzyl)-3,5-dimethyl-*N*-(2-((3-methylbenzyl)amino)-2-oxoethyl)benzamide 2q:** The hydroxamic acid was obtained as described in the general procedure D using ester **12q** in 24 % yield as a white solid: mp = 114-118 °C; ^{1}H-NMR (DMSO-d_6, 300 MHz): δ [ppm] = 2.24 (s, 6 H), 2.28 (s, 3 H), 3.76/3.97* (2 x s, 2 H), 4.23-4.28 (m, 2 H), 4.51*/4.65 (2 x s, 2 H), 6.93-7.06 (m, 6 H), 7.17-7.33 (m, 3 H), 7.72-7.74 (m, 2 H), 8.36-8.45 (m, 1 H), 10.05 (brs, 1 H); ^{13}C-NMR (DMSO-d_6, 12 MHz): δ [ppm] = 20.6, 20.9, 42.1, 47.4, 48.5, 50.9, 53.1, 124.0, 124.2, 126.8, 127.0, 127.4, 127.5, 127.8, 128.1, 129.2, 130.7, 131.8, 135.9, 137.2, 137.4, 138.9, 139.0, 140.0, 140.3, 163.7, 167.6, 171.5; HRMS calculated for $C_{27}H_{29}N_3O_4$: 460.2231 $[M+H]^+$, found 460.2225; HPLC purity: 97.2 %.

***N*-(4-(Hydroxycarbamoyl)benzyl)-3,5-dimethyl-*N*-(2-oxo-2-((pyridin-3-ylmethyl)amino)ethyl)benzamide 2r:** The hydroxamic acid was obtained as described in the general procedure D using ester **12r** in 69 % yield as a reddish solid: mp = 138-139 °C; ^{1}H-NMR (DMSO-d_6, 600 MHz): δ [ppm] = 2.23 (s, 6 H), 3.79/3.99* (2 x s, 2 H), 4.29/4.35* (2 x d, J = 5.7, 5.4 Hz, 2 H), 4.56*/4.68 (2 x s, 2 H), 7.00-7.06 (m, 3 H), 7.27-7.40 (m, 3 H), 7.56-7.67 (m, 1 H), 7.73-7.75 (m, 2 H), 8.43-8.52 (m, 3 H), 9.04 (s, 1 H), 11.21 (s, 1 H); ^{13}C-NMR (DMSO-d_6, 151 MHz): δ [ppm] = 20.8, 47.7, 48.7, 51.1, 53.3, 123.5, 124.0, 124.1, 126.9, 127.1, 127.2, 127.7, 130.9, 131.7, 134.6, 135.1, 136.0, 137.6, 140.5, 148.1, 148.2, 148.7, 148.8, 164.0, 168.0, 171.6; HRMS calculated for $C_{25}H_{26}N_4O_4$: 447.2027 $[M+H]^+$, found 447.2030; HPLC purity: 97.1 %.

***N*-(4-(Hydroxycarbamoyl)benzyl)-3,5-dimethyl-*N*-(2-(methylamino)-2-oxoethyl)benzamide 2s:** The hydroxamic acid was obtained as described in the general procedure D using ester **15s** in 40 % yield as a white solid: mp = 187-188 °C; ^{1}H-NMR (DMSO-d_6, 600 MHz): δ [ppm] = 2.23*/2.27 (2 x s, 6 H), 2.57/2.62* (2 x d, J = 4.3, 4.1 Hz, 3 H), 3.69/3.88* (2 x s, 2 H), 4.53*/4.64 (2 x s, 2 H), 7.02-7.07 (m, 3 H), 7.25-7.39 (m, 2 H), 7.72-7.74 (m, 2 H), 7.83-7.90 (m, 1 H), 9.04 (s, 1 H), 11.21 (s, 1 H); ^{13}C-NMR (DMSO-d_6, 151 MHz): δ [ppm] = 20.8, 25.5, 47.4, 48.5, 51.1, 53.1, 124.2, 126.9, 127.1, 127.3, 127.6, 130.8, 131.7, 131.9, 135.9, 136.0, 137.6, 140.3, 140.5, 164.0, 168.0, 168.2, 171.6; HRMS calculated for $C_{20}H_{23}N_3O_4$: 370.1761 $[M+H]^+$, found 370.1761, HPLC purity: 96.4 %.

***N*-(4-(Hydroxycarbamoyl)benzyl)-2-methyl-*N*-(2-(methylamino)-2-oxoethyl)benzamide 2t:** The hydroxamic acid was obtained as described in the general procedure D using **15t** in 86 % yield as a white solid: mp = 147-149 °C; ^{1}H-NMR (DMSO-d_6, 400 MHz): δ [ppm] = 2.23/2.31* (2 x s, 3 H), 2.52/2.63* (2 x d, J = 4.5, 4.5 Hz, 3 H), 3.59/3.91* (s and brs, 2 H), 4.38/4.68* (s and brs, 2 H), 7.16-7.31 (m, 5 H), 7.41-7.43 (m, 1 H), 7.69-7.86 (m, 3 H), 9.03 (s, 1 H), 11.07 (s, 1 H); ^{13}C-NMR (DMSO-d_6, 101 MHz): δ [ppm] = 18.58, 18.60, 25.5, 46.3, 47.9, 50.3, 52.2, 125.5, 125.60, 125.63, 125.66, 127.0, 127.15, 127.19, 127.8, 128.8, 130.2, 130.3, 131.8, 131.9, 134.1, 134.3, 135.9, 136.0, 139.8, 140.5, 163.9, 167.7, 167.9, 171.09, 171.12; HRMS calculated for $C_{19}H_{21}N_3O_4$: 356.1605 $[M+H]^+$, found 356.1608, HPLC purity: 97.4 %.

Biological evaluation

***P. falciparum* asexual intraerythrocytic culture and growth inhibition assays**

Asexual drug-sensitive *P. falciparum* parasites (3D7)[25a] were cultured *in vitro* in O+ human erythrocytes and RPMI 1640 media (Gibco, USA) containing 10% heat inactivated human serum and 5 µg/ml gentamycin (Sigma Aldrich, USA). Cultures were maintained at 37°C in 5% CO_2, 5% O_2, N_2 gas mixture. The [^{3}H]-hypoxanthine incorporation method was used to define *in vitro* growth inhibition, essentially as previously described [12a]. Briefly, ring-stage *P. falciparum* infected erythrocytes (0.25% final parasitemia, 2.5% haematocrit) were incubated in 96 well plates with serial dilutions of test compounds (dissolved in DMSO vehicle; ≤0.5% final DMSO concentration) or controls. After 48h incubation, [^{3}H]-hypoxanthine (0.5 µCi/well) was added and [^{3}H]-hypoxanthine incorporation assessed after a further 24h incubation. The 50% inhibitory concentration (IC_{50}) was calculated using linear interpolation of inhibition curves[25b]. A minimum of three independent assays were carried out, each in triplicate wells, and data presented as mean IC_{50} ± SD (standard deviation).

Protein hyperacetylation assays

Protein hyperacetylation assays were carried out essentially as previously described[14]. Briefly, synchronised trophozoite-stage *P. falciparum* 3D7 infected erythrocytes (3-5% parasitemia, 5% haematocrit, 3ml culture per well) were incubated with 5x IC_{50} of test compounds or controls. Controls included parasites treated with 5x IC_{50} vorinostat and DMSO vehicle control. Protein lysates were prepared via saponin lysis and resuspension of parasite pellets in 1x SDS-PAGE loading dye. Following heat denaturation (95ºC; 5min), proteins were analysed by SDS-PAGE and Western blot using PVDF membrane, anti-(tetra)acetyl histone H4 primary antibody (1:2,000 dilution; Merck Millipore, USA; known to cross-react with acetylated histone H2 forms; Millipore product manual) and IRDye 680 goat anti-rabbit as the secondary antibody (1:10,000 dilution; Li-Cor Biosciences). REVERT total Protein Stain® (Li-Cor Biosciences, USA) was used prior to immunoblotting to control for loading, as per the manufacturer's instructions. Reactions were carried out in Odyssey Blocking Buffer (Li-Cor Biosciences), as per manufacturer's instructions, and membranes imaged using an Odyssey Fc (Li-Cor Biosciences, USA) at 700 nm. The hyperacetylation profile was analysed by densitometry analysis using Image Studio Lite Version 5.2 software. Each Western density signal was normalised to its respective total protein loading control and the results were expressed as the fold change in relative density compared to the **3h-C** DMSO vehicle control (set to one). Data are mean (±) SD for three independent experiments.

Gametocytocidal activity (ATP bioluminescence assay)

Activity against mature stage V gametocytes of the *P. falciparum* strain NF54 was evaluated by an ATP bioluminescence assay as described previously[26a] with minor modifications[26b]. Gametocyte culture was initiated from synchronized parasites kept in complete culture medium supplemented with 5% human serum, starting at a hematocrit of 6% and parasitemia of 0.3%. Culture medium was changed daily without parasite dilution throughout the entire experiment. When the parasitemia reached 5%, the volume of the medium was doubled. From days 12 to 15, gametocyte cultures were treated with 50 mM *N*-acetyl-D-glucosamine (MP Biomedicals GmbH) to remove asexual stages of the parasite, and on day 15 or 16, the culture was purified by a NycoPrep 1.077 cushion density gradient and magnetic column separation to remove uninfected erythrocytes and enrich the gametocyte population. All tested compounds were dissolved in DMSO before further dilutions with complete culture medium was done. After purification, mature gametocytes (50,000 per well) were incubated for 48 hours with the respective compound before performance of the ATP based luminescence assay. To evaluate the gametocytocidal activity of the compounds a pre-screening based on 2 concentrations (5 µM and 500 nM) together with the control compounds epoxomycin, methylene blue and chlorotonil A with known gametocytocidal activity was performed. Of the most promising compounds a 2-fold serial dilution was done to determine the 50% inhibitory concentration (IC_{50}) by analysing the nonlinear regression of log concentration–response curves using the drc-package v0.9.0 of R v2.6.1[26c].

Activity against *P. berghei*-Luc EFF and HepG2 viability (*P. berghei*-Luc Liver stage and HepG2 cytotoxicity assays)

The liver stage activity against *P. berghei-Luc* (Pb-Luc) EEFs and toxicity to HepG2 cells were evaluated in Pb-Luc and HepG2 cytotoxicity bioluminescence assays as described previously[27a]. HepG2-A16-CD81EGFP cells, stably transformed to express a GFP-tetraspanin receptor CD81 fusion protein, were cultured at 37 °C and 5% CO_2 in culture media (DMEM with phenol red (Life Technology, CA), 10% FBS and 1x Pen Strep Glutamine (Life Technologies, CA)). For both, *P. berghei*-Luc and HepG2 cytotoxicity assays, 20-26 hour prior to Pb-Luc sporozoites infection, 5 µL HepG2-A16-CD81EGFP cells (~$6x10^5$ cells/mL in assay medium (DMEM without Phenol Red (Life Technologies, CA), 5% FBS, and 5x Pen Strep Glutamine (Life Technologies, CA)) were seeded into white, solid-bottom, 1536-well plates (custom GNF mold ref# 789173-F, Greiner Bio-One). Next 50 nL of compounds in 1:3 serial dilutions in DMSO (final DMSO concentration per well 0.5%) were transferred with an Acoustic Transfer System (ATS) (Biosero) instrument into the assay plates. Atovaquone (0.5 µM) and puromycin (10 µM) in 1:3 serial dilutions in DMSO were used as positive controls for Pb-Luc and HepG2 cytotoxicity assays, respectively. Wells containing 0.5% DMSO were used as negative controls for both assays. For Pb-Luc infection, *P. berghei*-ANKA-GFP-Luc-SMCON (Pb-Luc)[27b] sporozoites were freshly isolated from infected *A*nopheles *stephensi* mosquitoes (received from Insectary Core Facility at New York University). Dissected salivary glands were homogenized in DMEM media (Life Technology, CA) using a glass tissue grinder and filtered twice through a 20 µM nylon net filter (Steriflip, Millipore). The sporozoites were counted using a Neubauer hemocytometer (C-Chip, InCyto, Republic of Korea), adjusted to final concentration of 200 sporozoites per 1 µL in assay media, and placed on ice until needed. Next ~1,000 sporozoites (5 µL) were added to each well with a single tip Bottle Valve liquid handler (GNF). The assay plates were spun down at 37 °C for 3 minutes with a centrifugal force of 330xg on normal acceleration and brake setting. For the HepG2 cytotoxicity assay, 5 µL per well of additional assay media (but not sporozoites) was added to the HepG2-A16-CD81EGFP cells to maintain equal concentrations of

compounds relative to the Pb-Luc infected plates. Both sets of plates were incubated at 37 °C for 48 h in 5% CO_2 with high humidity to minimize media evaporation and edge effects. After incubation media was removed by spinning the inverted plates at 150xg for 30 seconds. Next, 2 µL per well of BrightGlo (Promega) for quantification of Pb-Luc EEFs or CellTiterGlo (Promega) reagent (diluted 1:2 with deionized water) for quantification of HepG2-A16-CD81EGFP cell viability were dispensed with the MicroFlo (BioTek) liquid handler. Luminescence was immediately measured using an Envision Multilabel Reader (PerkinElmer). For data analysis EEF inhibition background was defined as the average of the five highest atovaquone concentrations (20 wells), and the background for the HepG2 cytotoxicity was defined as the average of the 3 highest puromycin concentrations (12 wells). IC_{50} values were determined using the average normalized bioluminescence intensity of 4 wells per concentration and plate (96 wells in total for each compound) and a nonlinear variable slope four-parameter regression curve fitting model in Prism 6 (GraphPad Software Inc.).

In vitro testing on hHDAC1 and hHDAC6

The in vitro inhibitory activity of **2c-i, 2s-t** and **SAHA** against two human HDAC isoforms (1 and 6) were measured using a previously published protocol[22]. OptiPlate-96 black microplates (Perkin Elmer) were used with an assay volume of 50 µL. 5 µL test compound or control, diluted in assay buffer (50 mM Tris-HCl, pH 8.0, 137 mM NaCl, 2.7 mM KCl, 1 mM $MgCl_2$, 0.1 mg/mL BSA), were incubated with 35 µL of the fluorogenic substrate ZMAL (Z-(Ac)Lys-AMC)[28] (21.43 µM in assay buffer) and 10 µL of human recombinant HDAC1 (BPS Bioscience, Catalog# 50051) or HDAC6 (BPS Bioscience, Catalog# 50006) at 37 °C. After an incubation time of 90 min, 50 µL of 0.4 mg/mL trypsin in trypsin buffer (50 mM Tris-HCl, pH 8.0, 100 mM NaCl) were added, followed by further incubation at 37 °C for 30 min. Fluorescence was measured with an excitation wavelength of 355 nm and an emission wavelength of 460 nm using a Fluoroskan Ascent microplate reader (Thermo Scientific). All compounds were evaluated in duplicate in at least two independent experiments.

Acknowledgements

This work was supported by the Deutsche Forschungsgemeinschaft (DFG) (HA 7783/1-1 to FKH and HE 7607/1-1 to JH), E.A.W. is supported by grants from the NIH (5R01AI090141 and R01AI103058). E. H. is supported by Griffith University postgraduate scholarships. The Deutsche Forschungsgemeinschaft (DFG) is acknowledged for funds used to purchase the UHR-TOF maXis 4G, Bruker Daltonics, Bremen HRMS instrument used in this research. We acknowledge the Australian Red Cross Blood Service for the provision of human blood and sera for *P. falciparum* culture.

References:

[1] WHO, World Health Organization: World Malaria Report *WHO Press, Geneva* **2017**

[2] a) K. T. Andrews, T. N. Tran, D. P. Fairlie, *Curr. Pharm. Design* **2012**, *18,* 3467-3479; b) A. Bouchut, D. Rotili, C. Pierrot, S. Valente, S. Lafitte, J. Schultz, U. Hoglund, R. Mazzone, A. Lucidi, G. Fabrizi, D. Pechalrieu, P. B. Arimondo, T. S. Skinner-Adams, M. J. Chua, K. T. Andrews, A. Mai, J. Khalife, *Eur. J. Med. Chem.* **2019**, *161,* 277-291.

[3] a) B. Mordmüller, G. Surat, H. Lagler, S. Chakravarty, A. S. Ishizuka, A. Lalremruata, M. Gmeiner, J. J. Campo, M. Esen, A. J. Ruben, J. Held, C. L. Calle, J. B. Mengue, T. Gebru, J. Ibáñez, M. Sulyok, E. R. James, P. F. Billingsley, KC Natasha, A. Manoj, T. Murshedkar, A. Gunasekera, A. G. Eappen, T. Li, R. E. Stafford, M. Li, P. L. Felgner, R. A. Seder, T. L. Richie, B. K. L. Sim, S. L. Hoffman, P. G. Kremsner, *Nature* **2017**, *542*, 445-449; b) RTS,S Clinical Trials Partnership, Efficacy and safety of RTS,S/AS01 malaria vaccine with or without a booster dose in infants and children in Africa: final results of a phase 3, individually randomised, controlled trial, *Lancet* **2015**, *386*, 31-45.

[4] World Health Organization. Malaria vaccine: WHO position paper – January 2016. *The Weekly Epidemiological Record* (*WER*) **2016**, *91*, 33-52.

[5] K. Stenzel, M. J. Chua, S. Duffy, Y. Antonova-Koch, S. Meister, A. Hamacher, M. U. Kassack, E. Winzeler, V. M. Avery, T. Kurz, K. T. Andrews, F. K. Hansen, *ChemMedChem* **2017**, *12*, 1627-1636.

[6] C. Wongsrichanalai, C. H. Sibley, *Clin. Microbiol. Infect.* **2013**, *19*, 908-916.

[7] K. T. Andrews, A. Haque, M. K. Jones, *Immunol. Cell Biol.* **2012**, *90*, 66-77.

[8] M. Mottomal, S. Zheng, T. L. Huang, G. Wang, *Molecules* **2015**, *20*, 3898-3941.

[9] A. Didonna, P. Opal, *Ann. Clin. Transl. Neurol.* **2015**, *2*, 79-101.

[10] A. Villagra, E. M. Sotomayor, E. Seto, *Oncogene* **2010**, *29*, 157-173.

[11] a) M. New, H. Olzscha, N. B. La Thangue, *Mol. Oncol.* **2012**, *6*, 637-656; b) A. Kanyal, M. Rawat, P. Gurung, D. Choubey, K. Anamika, K. Karmodiya, *The FEBS Journal* **2018**, *286*, 1767-1782.

[12] a) K. T. Andrews, T. N. Tran, A. J. Lucke, P. Kahnberg, G. T. Le, G. M. Boyle, D. L. Gardiner, T. S. Skinner-Adams, D. P. Fairlie, *Antimicrob. Agents Chemother.* **2008**, *52*, 1454-1461; b) M. J. Chua, M. S. J. Arnold, W. Xu, J. Lancelot, S. Lamotte, G. F. Späth, E. Prina, R. J. Pierce, D. P. Fairlie, T. S. Skinner-Adams, K. T. Andrews, *Int. J. Parasitol. Drugs Drug Resist.* **2017**, *7*, 42-50.

[13] a) J. Melesina, D. Robaa, R. J. Pierce, C. Romier, W. Sippl, *J. Mol. Graph. Model.* **2015**, *62*, 342-361; b) G. S. Hailu, D. Robaa, M. Forgione, W. Sippl, D. Rotili, A. Mai, *J. Med. Chem.* **2017**, *60*, 4780-4804.

[14] J. A. Engel, A. J. Jones, V. M. Avery, S. D. Sumanadasa, S. S. Ng, D. P. Fairlie, T. S. Adams, K. T. Andrews, *Int. J. Parasitol. Drug Drug Resist.* **2015**, *5*, 117-126.

[15] K. T. Andrews, A. P. Gupta, T. N. Tran, D. P. Fairlie, G. N. Gobert, *PLoS One* **2012**, *7*, e31847.

[16] a) S. J. Darkin-Rattray, A. M. Gurnett, R. W. Myers, P. M. Dulski, T. M. Crumley, J. J. Allocco, C. Cannova, P. T. Meinke, S. L. Colletti, M. A. Bednarek, S. B. Singh, M. A. Goetz, A. W. Dombrowski, J. D. Polishook, Dennis M. Schmatz, *Proc. Natl. Acad. Sci USA* **1996**, *93*, 13143-13147; b) Y. Chen, M. Lopez-Sanchez, D. N. Savoy, D. D. Billadeau, G. S. Dow, A. P. Kozikowski, *J. Med. Chem.* **2008**, *51*, 3437-3448.

[17] D. Diedrich, K. Stenzel, E. Hesping, Y. Antonova-Koch, T. Gebru, S. Duffy, G. Fisher, A. Schöler, S. Meister, T. Kurz, V. M. Avery, E. A. Winzeler, J. Held, K. T. Andrews, F. K. Hansen, *Eur. J. Med. Chem.* **2018**, *158*, 801-813.

[18] a) S. D. Sumanadasa, C. D. Goodman, A. J. Lucke, T. Skinner-Adams, I. Sahama, A. Haque, T. A. Do, G. I. McFadden, D. P. Fairlie, K. T. Andrews, *Antimicrob. Agents Chemother.* **2012**, *56*, 3849-3856; b) F. K. Hansen, S. D. Sumanadasa, K. Stenzel, S. Duffy, S. Meister, L. Marek, R. Schmetter, K. Kuna, A. Hamacher, B. Mordmüller, M. U. Kassack, E. A. Winzeler, V. M. Avery, K. T. Andrews, T. Kurz, *Eur. J. Med. Chem.* **2014**, *82*, 204-2013; c) F. K. Hansen, T. S. Skinner-Adams, S. Duffy, L. Marek, S. D. Sumanadasa, K. Kuna, J. Held, V. M. Avery, K. T. Andrews, T. Kurz, *ChemMedChem* **2014**, *9*, 665-670; d) K. Trenholme, L. Marek, S. Duffy, G. Pradel, G. Fisher, F. K. Hansen, T. S. Skinner-Adams, A. Butterworth, C. J. Ngwa, J. Moecking, C. D. Goodman, G. I. McFadden, S. D. M. Sumanadasa, D. P. Fairlie, V. M. Avery, T. Kurz, K. T. Andrews, *Antimicrob. Agents Chemother.* **2014**, *58*, 3666-3678.

[19] a) R. De Vreese, C. de Kock, P. J. Smith, K. Chibale, M. D'hooghe, *Future Med. Chem.* **2017**, *9*, 357-364; b) O. Witt, H. E. Deubzer, T. Milde, I. Oehme, *Cancer Lett.* **2009**, *277*, 8-21.

[20] a) D. Diedrich, A. Hamacher, C. G. Gertzen, L. A. Alves Avelar, G. J. Reiss, T. Kurz, H. Gohlke, M. U. Kassack, F. K. Hansen, *Chem. Commun.* **2016**, *52*, 3219-3222; b) N. J. Porter, J. D. Osko, D. Diedrich, T. Kurz, J. M. Hooker, F. K. Hansen, D. W. Christianson, *J. Med. Chem.* **2018**, *61*, 8054-8060; c) V. Krieger, A. Hamacher, C. G. W. Gertzen, J. Senger, M. R. H Zwinderman, M. Marek, C. Romier, F. J. Dekker, T. Kurz, M. Jung, H. Gohlke, M. U. Kassack, F. K. Hansen, *J. Med. Chem.* **2017**, *60*, 5493-5506.

[21] M. C. Pirrung, S. Ghorai, *J. Am. Chem. Soc.* **2006**, *128*, 11772-11773.

[22] M. K. W. Mackwitz, A. Hamacher, J. D. Osko, J. Held, A. Schöler, D. W. Christianson, M. U. Kassack, F. K. Hansen, *Org. Lett.* **2018**, *20*, 3255-3258.

[23] N. Reßing, V. Marquardt, C. G. W. Gertzen, A. Schöler, A. Schramm, T. Kurz, H. Gohlke, A. Aigner, M. Remke, F. K. Hansen, *MedChemComm* **2018**, DOI: 10.1039/C8MD00454D.

[24] Q. Lu, D.-S. Wang, C.-S. Chen, Y.-D. Hu, C.-S. Chen, *J. Med. Chem.* **2005**, *48*, 5530-5535.

[25] a) D. Walliker, I. A. Quakyi, T. E. Wellems, T. F. McCutchan, A. Szarfman, W. T. London, L. M. Corcoran, T. R. Burkot, R. Carter, *Science* **1987**, *236*, 1661–1666. b) W. Huber, J. C. Koella, *Acta Trop.* **1993**, *55*, 257-261.

[26] a) J. Lelièvre, M. J. Almela, S. Lozano, C. Miguel, V. Franco, D. Leroy, E. Herreros, *PLoS One* **2012**, *7*, e35019. b) T. Gebru, B. Mordmüller, J. Held, *Antimicrob. Agents Chemother.* **2014**, *58*, 7398-7404. c) R Core Team, R: a Language and Environment for Statistical Computing, R Foundation for Statistical Computing, Vienna, Austria, 2015. URL, https:// www.R-project.org/.

[27] a) J. Swann, V. Corey, C. A. Scherer, N. Kato, E. Comer, M. Maetani, Y. Antonova-Koch, C. Reimer, K. Gagaring, M. Ibanez, D. Plouffe, A. M. Zeeman, C. H. Kocken, C. W. McNamara, S. L. Schreiber, B. Campo, E. A. Winzeler, S. Meister, *ACS Infect. Dis.* **2016**, *2*, 281-293. b) B. Franke-Fayard, C. J. Janse, M. Cunha-Rodrigues, J. Ramesar, P. Buscher, I. Que, C. Lowik, P. J. Voshol, M. A. den Boer, S. G. van Duinen, M. Febbraio, M. M. Mota, A. P. Waters, *Proc. Natl. Acad. Sci. U.S.A.* **2005**, *102*, 11468-11473.

[28] B. Heltweg, F. Dequiedt, E. Verdin, M. Jung, *Anal. Biochem.* **2003**, *319*, 42-48.

Entry for the Table of Contents

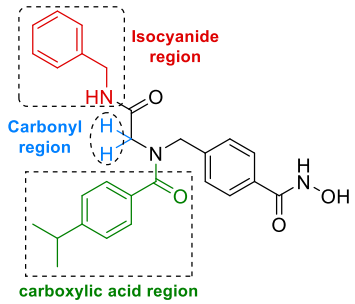

2h

IC_{50}(*Pf* 3d7): 0.0052 µM (SI: 889)
IC_{50}(*Pb* EEF): 0.016 µM (SI: 289)

The synthesis and biological evaluation of a series of novel peptoid-based HDACi is presented. All compounds were screened for activity against three different malaria parasite life cycle stages as well as for mammalian cell toxicity to investigate the structure-activity and structure-toxicity relationships of this class of antiplasmodial HDACi. Compound **2h** was identified as a parasite-selective HDACi with potent dual-stage antiplasmodial activity.